2005

A Novel Binding Interaction For The Paxillin Ld3 Motif: Paxillin Ld3 Mediates Merlin-Paxillin Binding At Paxillin Binding Domain 1

Sandra E. Beattie Geden
University of Central Florida

A NOVEL BINDING INTERACTION FOR THE PAXILLIN LD3 MOTIF: PAXILLIN LD3 MEDIATES MERLIN-PAXILLIN BINDING AT PAXILLIN BINDING DOMAIN 1

by

SANDRA E. BEATTIE GEDEN
B.S. University of Florida, 1989

A thesis submitted in partial fulfillment of the requirements
for the degree of Master of Science
in the Department of Molecular Biology and Microbiology
in the Burnett College of Biomedical Sciences
at the University of Central Florida
Orlando, Florida

Summer Term
2005

ABSTRACT

Neurofibromatosis type 2, an autosomal dominant genetic disorder, causes predisposed individuals to develop various benign central and peripheral nervous system tumors. The characteristic tumors of this disease are schwannomas, which are tumors of the Schwann cells, typically on the vestibular nerve. These and the other associated tumors slowly compress nervous system structures causing deafness and loss of balance, resulting in an average life-span of less than 40 years. The product of the *Nf2* gene is the protein named merlin or schwannomin. In individuals diagnosed with NF2, merlin is either absent or mutated to the point of inactivation. As such, merlin functions as a negative growth regulator in that it suppresses tumor growth. Being that NF2 is predominately a disease of the Schwann cells, merlin's functional role within the signal transduction pathways of Schwann cell growth and differentiation are being investigated. This thesis explores the molecular relationships between merlin and its various interactors within Schwann cells, and illuminates one step in elucidating merlin's functional mechanism of action. Merlin has been shown to associate with paxillin in a density-dependant manner and to bind directly to paxillin through two specific paxillin binding domains. Individual paxillin LD domain fusion proteins were produced, as well as recombinant merlin lacking the paxillin binding domains. Direct binding assays were performed in order to determine which specific paxillin domains merlin might interact with directly. The results indicate that, *in vitro*, merlin binds, through its PBD1 domain, to the paxillin LD3 motif. Supporting this

data, the results also demonstrate that when the merlin PBD1 domain is deleted, merlin binding to paxillin LD3 is abrogated. The direct binding shown here between paxillin and merlin, coupled with research demonstrating that merlin is present in β1 integrin immuno-precipitations, leads to the question of whether merlin binds directly to β1 integrin or associates with β1 integrin through paxillin. Using direct binding assays, this research shows that the merlin C-terminus binds directly to the cytoplasmic domain of β1 integrin, *in vitro*. Lastly, since merlin is an ERM family protein and has been shown to dimerize with ezrin (another ERM family member), and because merlin has been shown to bind directly to paxillin, the question asked is whether paxillin can interact directly with ezrin. The results indicate that paxillin can bind directly to the N-terminus of ezrin, *in vitro*. The findings presented here, when examined together, provide a framework for the proposal of a model in which paxillin LD3 mediates the localization of merlin to the plasma membrane, where it associates with the β1 integrin cytoplasmic domain and ezrin. These results and the proposed model offer additional insight into the mechanism of action of merlin's negative growth regulating function in Schwann cells.

ACKNOWLEDGMENTs

First and foremost, I would like to thank my husband, Mike Geden, for his loving support throughout my extensive "career change". Mike, I promise I won't go back to school for a PhD… at least until I'm 55! Thanks also go to my children, Daniel and Alex, for putting up with a mother who kept saying, "I can't, I have to study", or, "Not now, I have to go to the lab." I love you guys and I apologize for the missed time. Amazingly enough, both boys want to be scientists when they grow up. Many thanks go to my lab mates Marga Bott and Jared Iacovelli. In addition to answering my chemistry questions, Marga provided friendship and emotional support. And, although Jared and I sat back to back, I often used him as a sounding board for experiment ideas and as a double-checker on my calculations when I was just too tired to think straight. I would also like to thank Dr. Lucia Cilenti for all her guidance and for her considerable patience in answering my too-numerous-to-count questions, and Kathleen Nemec also deserves a round of thanks for her unflappable emotional support throughout the years. Special thanks go out to JoAnn Licht and Judy Gerrard for their friendship and spiritual support; I couldn't have finished it without you. Finally, I would like to acknowledge my advisor, Dr. Cristina Fernandez-Valle. Dr. Valle has an amazingly sharp mind, and I can only hope to acquire the memory for scientific detail that she posseses. Thank you, Dr. Valle, for the privilege of working in your lab.

TABLE OF CONTENTS

LIST OF FIGURES

LIST OF TABLES

INTRODUCTION

The long-term goal of the research conducted for this thesis is to understand the tumor growth-suppression function of the *Nf2* gene product, the protein merlin, in the etiology of the disease Neurofibromatosis Type 2. In general, this thesis research investigates the interactions between merlin and various proteins within the context of merlin's role in the signal transduction pathways of Schwann cells, the cell type predominantly affected in Neurofibromatosis Type 2.

An overview of Schwann cell biology, focal adhesions, and integrins is presented first in the Literature Review, followed by a summary of the clinical, genetic, and molecular aspects of Neurofibromatosis Type 2. Subsequent sections provide detailed background information concerning each protein relevant to this thesis research. Lastly, previous research and results obtained from this lab are discussed, leading to a statement of the specific aims for this thesis research.

Following the Literature Review, the Materials and Methods section lists all pertinent materials utilized for this research, as well as the methods employed to conduct these experiments. The individual results obtained for each question listed in the Specific Aims are presented in the Results section. To finish, the Discussion section presents an examination of the results, including conclusions and a proposed model detailing the interactions between merlin, paxillin, β1 integrin, and ezrin.

LITERATURE REVIEW

Schwann Cell Biology: Differentiation

The majority of cells present within any nervous system are the non-neural cells known as glia. Within vertebrate nervous systems, four major glial cell types are recognized; these are astrocytes, microglial cells, oligodendrocytes, and Schwann cells (SCs). The first three cell types are found only in the central nervous system (brain and spinal cord), while SCs are found only in the peripheral nervous system.

Development of the vertebrate peripheral nervous system is regulated by a series of complex interactions between the outgrowing neuronal axons and the developing SCs (Maurel and Salzer, 2000). SCs begin their existence as a transient group of cells, known as neural crest cells, which migrate out from the neural tube at the initiation of embryonic development (Haack and Hynes, 2001). During embryonic growth, a sub-population of the neural crest cells begins migrating along pre-existing axon tracts on the developing peripheral nerve trunks (Bunge and Fernandez-Valle, 1995). Throughout embryogenesis, the neural crest cells consecutively differentiate into two intermediate cell types; first into SC precursor cells, then into immature SCs (Jessen and Mirsky, 2002). At this point in development, the survival, proliferation, and differentiation of these intermediate cell

types is extremely dependent upon many signaling factors, such as contact-dependent mitogens derived from the axons (Garratt et al., 2000; Zanazzi et al., 2001). In one study, mice with specific disruptions of the neuregulin-1 gene exhibited a major shortage of precursor SCs (Meyer and Birchmeier, 1995). A severe deficiency in this cell type affects the developing neurons, as adequate precursor SCs are required for neuronal survival (Scherer, 2002).

As the SC precursors differentiate into immature SCs, they begin to surround large bundles of axons. In a process termed radial sorting, the axons are penetrated by thin SC cytoplasmic processes that segregate the axons into smaller and smaller bundles (Feltri et al., 2002). Concurrent with the sorting, the evolving SCs deposit a specialized form of extracellular matrix known as basal lamina (Scherer, 2002). As the sorting process continues, bundles of smaller diameter axons remain enveloped by cords of immature SCs (Scherer, 2002). These are the cells that, with maturation, become ensheathing SCs.

As the immature SCs actively compete for axonal domain, segments of the larger diameter axons become individually surrounded by a single immature SC (Bunge and Fernandez-Valle, 1995). Competition for axonally-derived trophic factors guarantees that the number of immature SCs produced is sufficient for the number of axons present and for their length. When the appropriate quantity of immature SCs has been generated, around the time of birth, the axons, together with their layer of basal lamina, induce SC differentiation (Zanazzi et al., 2001). The immature SCs differentiate into one of two mature SC types; these are known as myelinating, which arise first, and non-myelinating, also called ensheathing, which develop later (Mirsky et al., 2002).

Myelinating SCs form the myelin sheath, which is an important feature of motor and sensory neurons within the peripheral nervous system, as it acts as an electrical insulator. This allows for the extremely rapid conduction of nerve impulses due to a lowering of the axonal membrane capacitance. Proper myelination occurs only when SCs have deposited an organized basal lamina, which is a specialized type of extracellular matrix (ECM) (Schuppan et al., 1994). Studies show that interference with synthesis of SC basal lamina disrupts myelination (Fernandez-Valle et al., 1994; Feltri et al., 2002). Formation of a myelin segment commences when a mature SC advances one lip of its encircling membrane under the opposing lip of the cell. The underlying edge of the membrane continues to force itself under the overlying SC cytoplasm and around the axon until a compact myelin sheath results (reviewed in Bunge and Fernandez-Valle, 1995).

Focal Adhesions and Integrins

Focal adhesions (FAs) are specialized areas of tight attachment between a cell and its underlying ECM where integrin receptors link the actin cytoskeleton to the ECM (Sastry and Burridge, 2000). As such, FAs provide a structural link between the actin cytoskeleton and the ECM for the purpose of adhesion and motility (Burridge and Chrzanowska-Wodnicka, 1996). In addition, FAs are sites of signal propagation and transduction that have an influence on basic cellular functions such as growth control and apoptosis (Woodrow et al., 2003). A FA complex consists of the ECM components such

as collagens, noncollagenous glycoproteins (laminin, fibronectin), and proteoglycans, the cytoplasmic components such as actin, FAK (focal adhesion kinase), and paxillin, and lastly, the transmembrane components (Schuppan et al., 1994).

The major transmembrane components of FAs are integrins, which are a large family of heterodimers composed of α and β subunits (Schuppan et al., 1994; Previtail et al., 2001). Figure 1 illustrates the structure of integrin heterodimers. There are at least 18 variants of the integrin α subunit and 8 variants of the β subunit, therefore a variety of heterodimers can be formed which promote integrin diversity (Lee and Juliano, 2002). Integrins are composed of a large extracellular head domain responsible for ligand binding, a single-pass transmembrane segment, and, in all cases except one (the β4 chain), a short cytoplasmic tail of less than 50 amino acids (Liu et al., 2000; Liddington, 2002; Hynes, 2002). Integrins play a major role in cell adhesion and migration, and they exert control over cell differentiation, proliferation, and apoptosis (Liu et al., 2000).

Integrins mediate the transduction of signals through the cell membrane in both directions. "Outside-in" signaling occurs when extracellular ligands bind to the heterodimeric head triggering conformational changes which lead to a separation of the cytoplasmic tails (Hynes, 2003). This, in turn, allows the tails to bind intracellular proteins which then propagate the transmission of signals into the cell resulting in cellular differentiation, gene expression, and cytoskeletal reorganization (Liu et al., 2000; Liddington, 2002). "Inside-out" signaling, on the other hand, occurs when cytosolic proteins bind to one of the integrin cytoplasmic tails. This binding triggers a conformational change in the integrin extracellular head, resulting in a high-affinity active integrin. Integrin activation is depicted in Figure 2. Interestingly, paxillin is one

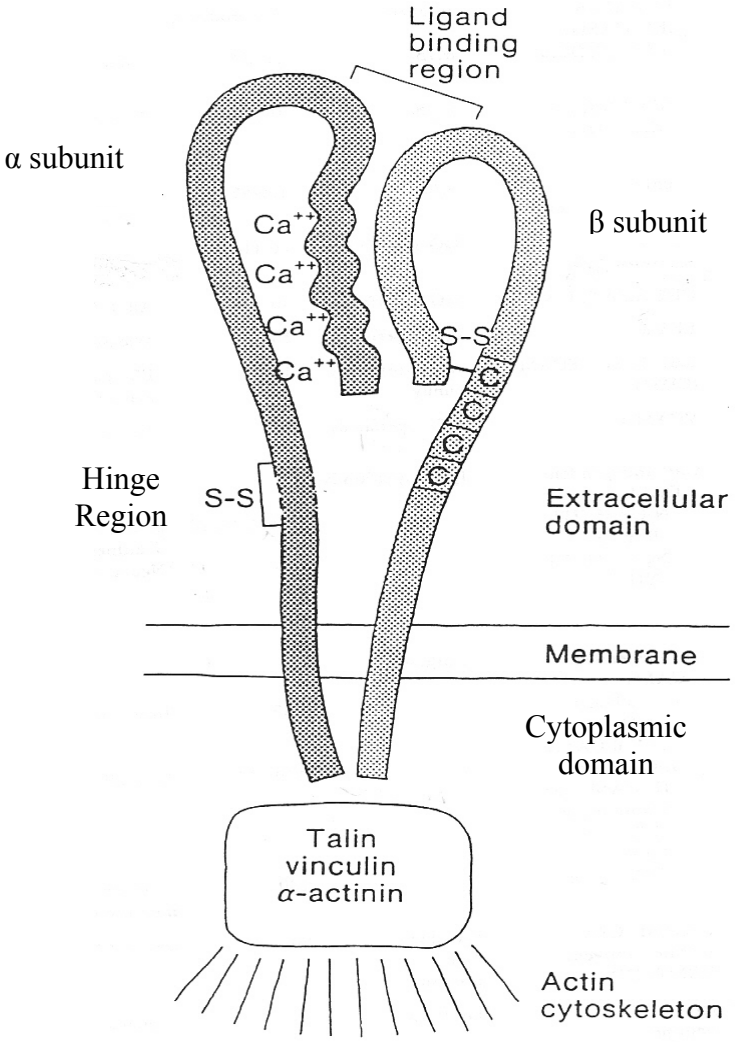

Figure 1. Structure of Typical Integrin.
Integrins are composed of two non-covalently associated α and β subunits. The extracellular domain contains the ligand binding region. The cytoplasmic domains of both subunits are relatively small and contain regions capable of binding various molecules, such as the cytoskeleton protein talin. Adapted from Albelda & Buck, 1990.

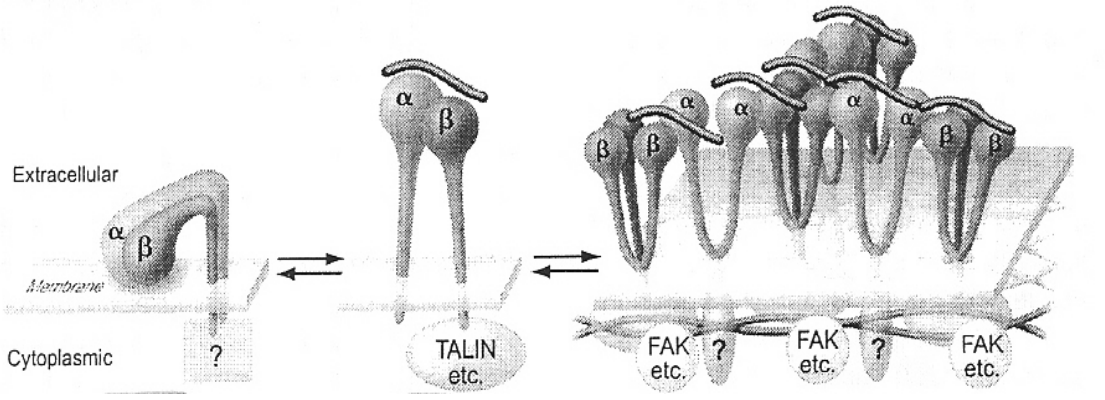

Figure 2. Depiction of Integrin Activation.
(Left) In the inactive state, the αβ heterodimer is bent over and does not bind to its extracellular ligands. (Middle) When activated, the αβ heterodimer is stablilized either by its extracellular ligand or by intracellular cytoskeleton protein binding, such as talin. (Right) Clustering of integrins leads to the formation of a signaling complex. Adapted from Hynes, 2003.

of the earliest proteins to be recruited to FAs in the leading edge of ruffling cells, and it only becomes tyrosine phosphorylated after integrin ligand binding (Lamorte et al., 2003). Tyrosine phosphorylation of paxillin has been shown to be essential for FA formation and the reorganization of the actin cytoskeleton (Lamorte et al., 2003).

Specifically, β1 integrin plays an important role in SCs. In immature and promyelinating SCs, the α6β1 integrin is expressed, while myelinating SCs mainly express α6β4 integrin (Previtali et al., 2001). Immature SCs require β1 integrin to properly segregate axons during development, and promyelinating SCs require β1 integrin to adhere to their basal laminae in order to initiate the formation of the myelin sheath (Scherer, 2002).

More to the point, β integrin cytoplasmic tails, with their NPXY consensus motif, have been shown to be essential for the correct subcellular localization of integrins and for the regulation of the affinity of integrins for their ligands (Liu et al., 2000). Additionally, β1 integrin cytoplasmic tails have been shown to be necessary for the activation of signaling pathways (Liu et al., 2000). As seen in Figure 3, the β1 integrin cytoplasmic domain, in particular, exhibits a wide variety of binding partners which range from actin-binding proteins such as talin, to signaling proteins such as the kinases ILK and FAK, and lastly, to miscellaneous proteins such as the adaptor protein paxillin (Liu et al., 2000). The β1 integrin cytoplasmic domain has also been shown to interact with merlin in isolated and differentiating SCs, and during differentiation paxillin and FAK assemble into a β1 integrin multi-molecular complex induced by basal lamina adhesion (Obremski et al., 1998; Chen et al., 2000).

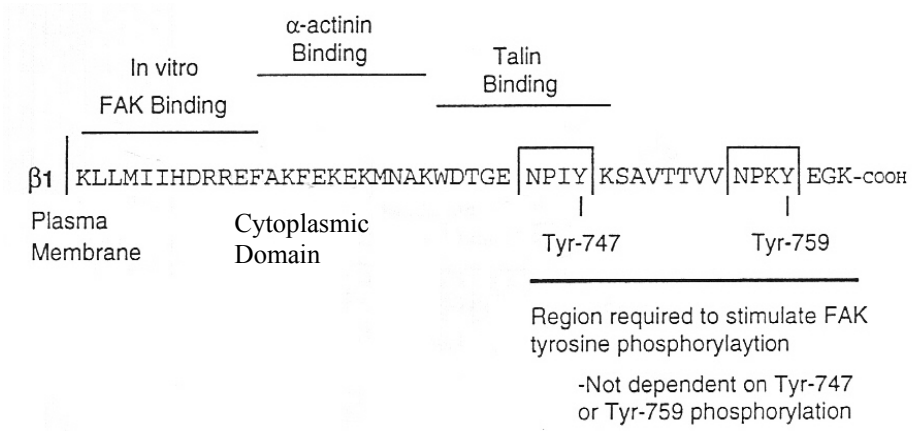

Figure 3. β1 Integrin Cytoplasmic Domain.
Locations of various binding partners are displayed. Note the NPXY motifs, which are important for integrin-mediated FAK association and activation. Adapted from Schlaepfer *et al.*, 1999.

Neurofibromatosis Type 2

Neurofibromatosis type 2 (NF2), formerly named central or bilateral acoustic neurofibromatosis (Brockes, 1986), is an autosomal dominant genetic disorder caused by the bi-allelic inactivation of the *Nf2* gene. Any children of an affected individual have a 50 percent risk of tumor formation (Martuza and Eldridge, 1988). The hallmark criterion for diagnosis of NF2 is the development of bilateral SC tumors, or schwannomas, on the vestibular branch of the eighth cranial nerves, those responsible for hearing (Rouleau et al., 1990). Accordingly, the first symptom of NF2 is usually hearing loss (Martuza and Eldridge, 1988). In addition to schwannomas, individuals with NF2 are predisposed to the development of various central nervous system (CNS) tumors such as meningiomas, spinal neurofibromas, ependymomas, and gliomas (Gutmann et al., 1997). The majority of these tumors are benign; with less than 1% ever undergoing malignant transformation (Wagner, 2003). Growth of these various NF2-associated tumors can cause a number of symptoms such as vertigo and paralysis, as well as extreme pain caused by the compression of nervous system structures over time (Rouleau et al., 1990; Martuza and Eldridge, 1988). The NF2 disorder affects between 1 in 33,000 to 40,000 live births (Ruggieri and Huson, 1999; Pykett et al., 1994), and the average life-span of affected individuals is typically less than 40 years (Gusella et al., 1999).

The gene suspected of involvement in the NF2 disorder was localized to chromosome 22 by the use of genetic linkage analysis and deletion mapping of both hereditary and sporadic schwannomas (acoustic neuromas) and meningiomas from NF2 patients (Seizinger et al., 1986; Seizinger et al., 1987a; Seizinger et al., 1987b; Dumanski

et al., 1987). These same studies suggested that the *NF2* locus encoded a tumor suppressor gene. A mutation in a tumor suppressor gene inactivates that gene's protein product, which normally aids in the inhibition of cell proliferation. Unregulated cell growth consequentially occurs, resulting in tumor formation. Subsequent cytogenetic research narrowed the location of the purported *NF2* gene to within the q12 region of chromosome 22 (Rouleau et al., 1987; Wertelecki et al., 1988; Rouleau et al., 1990; Narod et al., 1992; Wolff et al., 1992; Frazer et al., 1992). This same research additionally supported the theory of a tumor suppressor gene associated with the etiology of NF2. Studies were able to show that NF2 patients, with an inherited mutant allele of the purported *NF2* gene, were predisposed to tumor formation, occurring as a direct result of a somatic mutation in the remaining wild type allele (Hovens and Kaye, 2001).

In 1993, two independent research groups definitively identified the *NF2* gene through the use of positional cloning and chromosome walking. Both groups declared that the predicted protein product of this gene showed significant sequence homology to the ERM (ezrin-radixin-moesin) proteins (Bretscher et al., 2000). One group named this novel protein merlin (moesin, ezrin, and radixin-like protein) due to its similarity to the ERM proteins, while the other group named the protein product schwannomin, from schwannoma – the predominant tumor type seen in NF2 patients (Trofatter et al., 1993; Rouleau et al., 1993).

Merlin

Merlin is composed of 17 exons that, with alternative splicing, generate two major isoforms. As seen in Figure 4, isoform I consists of 595 amino acids and is encoded by exons 1 through 15 and 17. Isoform II, a 590 amino acid protein, is encoded by exons 1 through 16 and is identical to isoform I over the first 579 residues (Bianchi et al., 1994). The presence of exon 16 in isoform II results in a modified carboxy terminus (C-term) due to the addition of 11 amino acids followed by a stop codon that prevents the translation of exon 17 (Gusella et al., 1996). Research has shown that mutations linked to the NF2 disorder occur throughout the entire *NF2* gene, with the exception of exons 16 and 17 (Sainio et al., 2000). The majority of *NF2* mutations are hypothesized to result in truncated merlin proteins (den Bakker et al., 2000), with these types of mutations being associated with the more severe forms of NF2 (Sainio et al., 2000). Milder forms of NF2 are associated with missense mutations, and several exon 2 missense mutations and in-frame deletions, which produce measurable but dysfunctional merlin proteins, have been identified (Fernandez-Valle et al., 2002; Gutmann et al., 1998).

Similar to the ERM proteins after which it was named, merlin is composed of three structural domains as depicted in Figure 4 (Shimizu et al., 2002). The amino (N)-terminal FERM [protein 4.1 (four point one), ERM] domain consists of residues 1 through 310, while residues 311 to 478 comprise a large α–helical region (Chishti et al., 1998). The unique C-terminal domain of isoform I, composed of residues 479 through 595, lacks the actin-binding region conserved among other ERM proteins (Xiao et al., 2003). Crystallographic analysis of the merlin FERM domain reveals that it is comprised

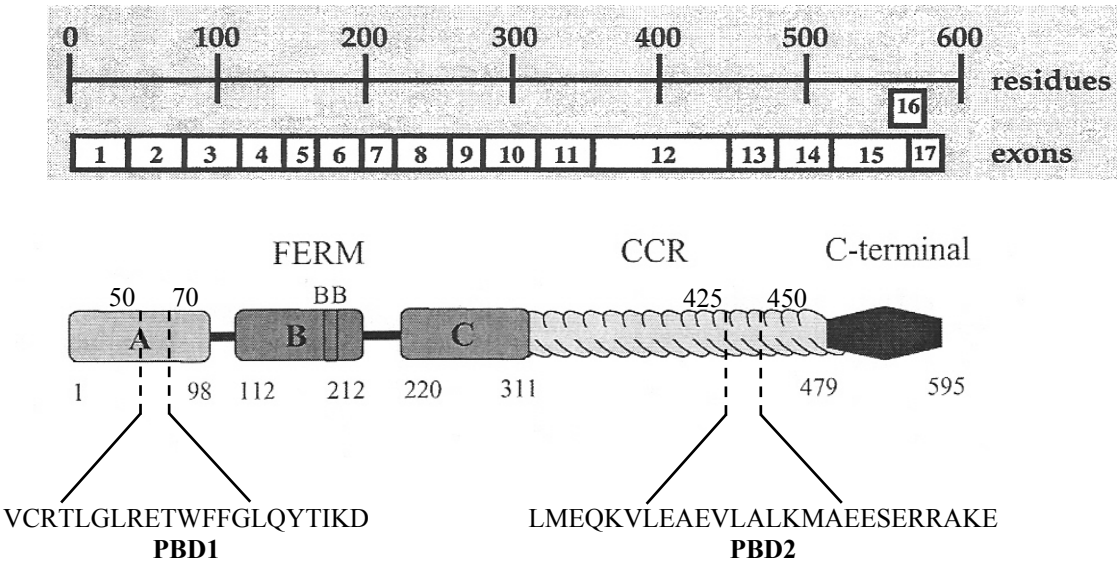

Figure 4. Merlin Structure with Corresponding Exons.
Merlin is composed of three major stuctural domains: the N-terminal FERM domain, the coiled-coil (CCR) or α-helical region, and the C-terminal tail. Note the locations of paxillin binding domains 1 (PBD1) and PBD2. Adapted from Sun *et al*., 2002 and Xu & Gutmann, 1998.

of three well-defined sub-domains, A, B, and C, which exhibit a three- dimensional cloverleaf structure (Sun et al., 2002). Present in sub-domain B is a run of 7 amino acids, residues 177 to 183, referred to as the Blue box (LaJeunesse et al., 1998). Although the Blue box region is identical in human merlin and the *Drosophila* homologue, it is not conserved among the other ERMs (LaJeunesse et al., 1998).

Research demonstrates that, similar to the ERM proteins, merlin isoform I is able to form two distinct intramolecular associations *in vitro* (Sherman et al., 1997; Gutmann et al., 1998). One such association transpires between the N-term and the C-term, specifically between residues 302-308 (within sub-domain C) and residues 580-595 (exon 17) (Gutmann et al., 1999). The other intramolecular association occurs between the extreme ends of the N-term itself, between sub-domains A and C, and is required for the stabilization of the N-term/C-term interaction (Gutmann et al., 1999). Because of its ability to associate intramolecularly, merlin isoform I can exist in two conformational states: closed and open (Gutmann et al., 1999). As depicted in Figure 5, the closed conformation is considered the active form and occurs through the N-term/C-term intramolecular association, while the open conformation is the inactive form (Gutmann, 2001). Studies show that the loss of just the final two C-terminal amino acids of merlin is enough to impair its self-association (Gutmann et al., 1999), thereby rendering the protein open and inactive.

Research has shown that merlin isoform I, which can self-associate, inhibits the growth of fibroblasts and RT4 rat schwannoma cells *in vitro* and *in vivo* (Lutchman and Rouleau, 1996; Sherman et al., 1997). Wild-type merlin typically localizes to the plasma membrane at areas rich in cortical actin, such as membrane ruffles (Gonzalez-Agosti et

Figure 5. Closed and Open Conformations of Merlin.
Merlin can adopt two conformations: closed and open. The closed conformation is the active tumor suppressor form, and the open conformation is the inactive or growth permissive form. Adapted from Martin *et al*., 2003.

al., 1996), and research has demonstrated that merlin can interact directly, *in vitro*, with actin (Deguen et al., 1998) through a unique N-terminal domain (residues 178-367) (Xu and Gutmann, 1998). LaJeunesse *et al.* have demonstrated that residues 177 to 183, the Blue box domain, of merlin are important for subcellular localization (LaJeunesse et al., 1998). Additionally, studies have shown that self-association of the merlin N-term is required for actin association and for the proper localization of merlin at the plasma membrane (Brault et al., 2001), and the N-term of merlin has been shown to localize, *in vitro*, to filopodia, cytoskeleton features, and the plasma membrane (Fernandez-Valle et al., 2002). Together, these data support the hypothesis that merlin's ability to alter its conformational state by intramolecular self-association, and by extension its localization, are critical to its function as a negative growth regulator (Sherman et al., 1997; Gutmann et al., 1998).

Past studies have suggested that merlin isoform II is unable to self-associate (Sherman et al., 1997; Gonzalez-Agosti et al., 1999) thus leading to the conclusion that merlin isoform II lacks tumor suppressor activity (Gutmann et al., 1998). More recently, however, research has demonstrated that isoform II does undergo intramolecular self-association, although in a uniquely different manner than that of isoform I, thereby suggesting that, while merlin isoform II doesn't function as a tumor suppressor, it does have unique functional properties (Scoles et al., 2002).

Various studies show that merlin's conformation alternates between the open (inactive) and closed (active) states in response to numerous factors, such as phosphorylation, and that these factors also contribute to its tumor suppressor activity (Sun et al., 2002). Western blot analysis of U2OS and NIH3T3 cells has demonstrated

that merlin isoform I is differentially phosphorylated as detected by the presence of a doublet (6% gel) at approximately 70 kDa (Shaw et al., 1998b). Specifically, the slower migrating form represents the phosphorylated merlin, while the faster migrating form represents the unphosphorylated merlin (Shaw et al., 1998b). Research suggests that unphosphorylated merlin most likely represents the active, and therefore closed, form of merlin (Shaw et al., 1998b). In support of this conclusion, recent studies show that merlin is phosphorylated on serine 518 (S518) by activated Rac/cdc42, and that this phosphorylation disrupts the merlin N-term/C-term self-association required for the active, i.e. growth suppressive, closed conformation (Shaw et al., 2001). Additional research, which utilized constitutively active forms of Rac/cdc42 kinase effectors and immunodepletion assays, reveals that merlin phosphorylation of S518 is induced specifically by PAK2, via activated Rac/cdc42, in NIH3T3 cells (Kissil et al., 2002). In support of this data, a recent study demonstrates that PAK2 directly phosphorylates wild-type merlin at S518, and additionally shows that this phosphorylation disrupts the merlin N-term/C-term self-association, *in vitro* and *in vivo* (Rong et al., 2004).

Ezrin: An ERM Family Member

The ERM family of proteins, which include ezrin, radixin, and moesin, belong to the protein 4.1 superfamily of membrane organizing proteins (Simons et al., 1998). All of this superfamily's members, of which merlin is one, share significant homology within the N-terminal FERM domain (Grönholm et al., 1999). The ERMs function as vital

cross-linkers between the actin cytoskeleton and the plasma membrane (Bretscher et al., 2000). As such, their interactions with both membrane proteins and the cortical actin cytoskeleton are essential for many basic cellular processes, including adhesion, motility, cell morphogenesis, cytokinesis, and transduction of growth signals for survival and proliferation (Gautreau et al., 2002; Bretscher et al., 2002).

Ezrin is a 13 exon protein with an apparent molecular weight of ~82 kDa (Bretscher et al., 2000; Tsukita and Yonemura, 1999). Like merlin, ezrin and its family members are composed of three major structural domains consisting of the FERM domain, a coiled-coil or α–helical region, followed by the C-terminal domain (Sun et al., 2002). The structure of ezrin is illustrated in Figure 6. Crystallographic analysis of the family's FERM domains reveals that, like merlin, ezrin and the ERMs are composed of three structural sub-domains, lobes F1, F2, and F3, which are analogous to merlin's sub-domains A, B, and C (Smith et al., 2003). While there are many similarities between merlin and ERM proteins, some key structural differences exist also. Ezrin and the ERM proteins possess an F-actin-binding site within the C-terminus, while merlin does not (Gusella et al., 1999). Additionally, merlin sub-domain B contains a stretch of 7 amino acids (residues 177 to 183) referred to as the Blue box, which is identical in human merlin and the *Drosophila* homologue, but which is not conserved among the ERMs (LaJeunesse et al., 1998).

Like merlin, ezrin and its ERM members can undergo intramolecular self-association in which the N-terminal domain binds to the C-terminal domain with high affinity (Bretscher et al., 2000). The ERMs can also associate intermolecularly by

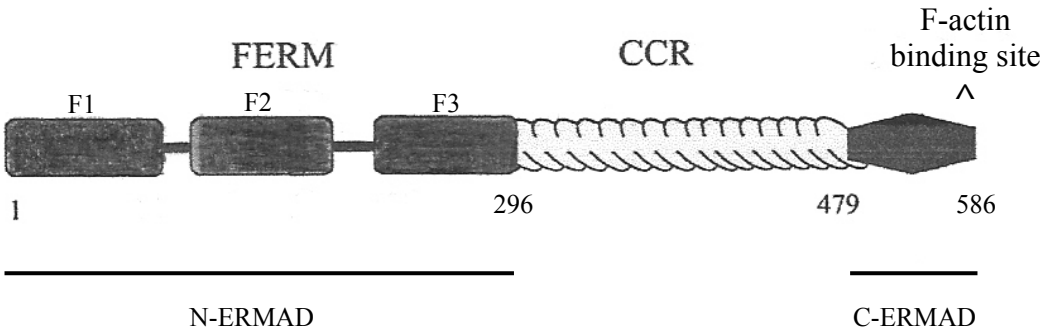

Figure 6. Structure of Ezrin.
Ezrin is composed of three major structural domains: the N-ERMAD or N-terminal FERM domain, the coiled-coil (CCR) or α-helical region, and the C-terminal C-ERMAD. Note the location of the F-actin binding domain. Adapted from Sun *et al*., 2002.

undergoing homotypic and heterotypic dimerization, through binding between their various N- and C-terminal domains (Bretscher et al., 2000). The discovery that the N-terminal domain of any ERM was able to bind to the C-terminal domain of any other ERM led these regions to be named N- and C-ERMAD for ERM association domain (Gary and Bretscher, 1995). In ezrin, the N-ERMAD was found to be coincident with the FERM domain, and this region encompasses amino acids 1 through 296 (Grönholm et al., 1999). The C-ERMAD of ezrin is composed of residues 479 through 585 (Gary and Bretscher, 1995).

Ezrin and the ERMs are negatively regulated by the conformational changes that occur as the result of their intramolecular and intermolecular associations (Bretscher et al., 2002). As such, ERM monomers are thought to be maintained in a closed or dormant conformation in which the N-ERMAD and C-ERMAD domains are in high affinity association with each other (Grönholm et al., 1999; Gautreau et al., 2002). In this inactive form, the C-ERMAD has an elongated tail which covers a large portion of lobes F2 and F3 of the FERM domain, thereby masking both the FERM domain binding sites and the C-ERMAD F-actin binding site (Pearson et al., 2000). Additionally, it has been suggested that homotypic and heterotypic ERM oligomers also represent inactive forms, as their head-to-tail intermolecular associations also mask their respective FERM and C-ERMAD binding sites (Grönholm et al., 1999).

As the dormant state of the ERMs is the closed conformation, it follows that the open conformation of ezrin and the ERMs requires that the FERM and C-ERMAD domains become separated. Studies show that multiple stimuli can activate the ERMs, and in all cases these stimuli result in ERM phosphorylation (Gautreau et al., 2002).

Research demonstrates that hyperphosphorylation of a corresponding threonine (T) residue within the C-terminal tail of all the ERMs (T567 in erzrin) was shown to significantly reduce the affinity of the C-ERMAD for the FERM domain, *in vitro* (Matsui et al., 1998). Rho kinase, protein kinase Cα (PKCα), and PKCθ are kinases which have been shown, both *in vitro* and *in vivo*, to phosphorylate the C-terminal ERM threonine (Bretscher et al., 2002). Specifically, ezrin phosphorylation by PKCθ, in the presence of lipids, has been shown to unmask the F-actin and EBP50 binding sites (Simons et al., 1998). Because the phosphorylation of ezrin occurs in the presence of phospholipids, it has been suggested that lipids may also be involved in ERM activation. In fact, one study suggests that the conserved threonine phosphorylation of ERMs may not be required at all for activation (Matsui et al., 1998). To further this hypothesis, Matsui et al. conducted additional research, the results of which suggest that PIP2 (phosphatidylinositol-4,5-bisphosphate) directly activates the ERMs by binding to the FERM domain, and that the activated ERM proteins are then phosphorylated at their C-terminal residue for stabilization (Matsui et al., 1999). In support of this theory, research shows that when the ERM PIP2 binding site is mutated, ezrin alters it localization from the membrane to the cytoplasm (Barret et al., 2000).

Paxillin

Paxillin is a 559-amino acid FA-associated adaptor protein with an apparent molecular weight of ~68 kDa (Tumbarello et al., 2002). It is highly conserved between

species, showing at least 90% identity between human and chickens, and it is abundantly expressed in a wide variety of tissues (Turner, 2000). In general, adaptor proteins, through their multi-domain structure, perform the essential task of facilitating transduction of both adhesion- and growth factor-dependent signals at the plasma membrane (Turner, 2000). Specifically, paxillin is thought to function as a scaffold for the recruitment of various cytoskeleton and signaling proteins to FA complexes, and there, to integrate these signals for transmission downstream (Schaller, 2001). The paxillin superfamily consists of paxillin, Hic-5, leupaxin, and PaxB, all of which share highly conserved domains within their N- and C-termini (Tumbarello et al., 2002). DALP, the death-associated LIM-only protein, is another member of the paxillin superfamily, but differs from the other members in that it is comprised solely of Lin-11, Isl-1, Mec-3 (LIM) domains (Turner, 2000).

As illustrated in Figure 7, the structure of paxillin is composed of two major domains; the N-terminus consisting of residues 1 through 325, and the C-terminus, which is composed of amino acids 326 to 559 (Turner, 2000). The paxillin N-terminus contains two sites for tyrosine phosphorylation (residues 31 and 118) which, when activated provide binding sites for Src homology 2 (SH2) domain-containing proteins (Brown et al., 1996). Additionally, the N-terminus provides binding sites various proteins such as FAK, vinculin, actopaxin, and SH3 domain-containing proteins (Brown et al., 1996; Nikolopoulos and Turner, 2000; Turner and Miller, 1994). The C-terminus of paxillin contains four consecutive LIM domains which serve as binding sites for various proteins such as PTP-PEST, tubulin, and other serine/threonine kinases (Shen et al., 1998; Cote et

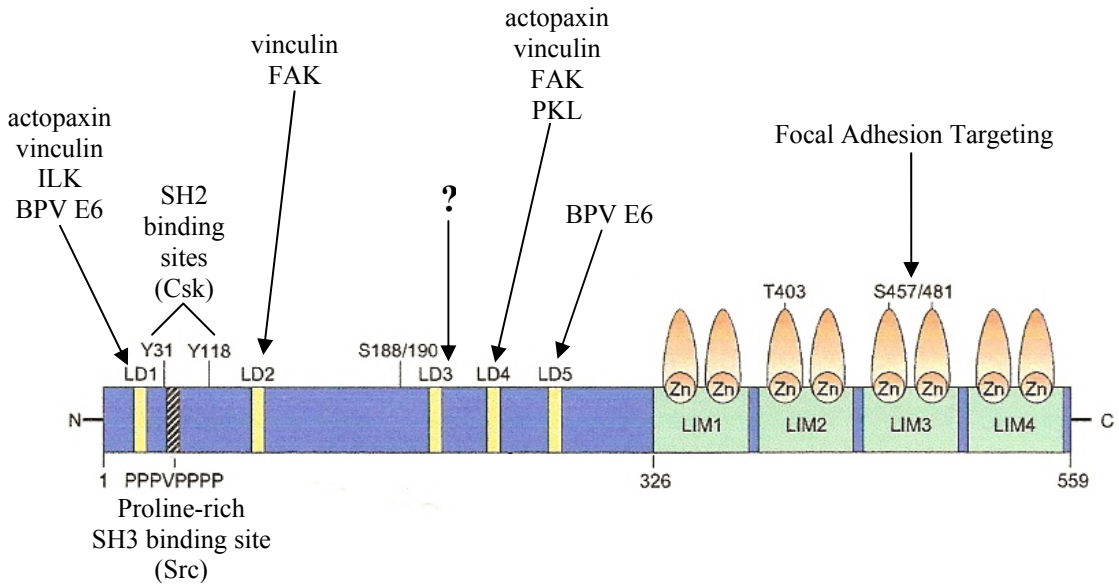

LD1: ^{4}LD A LL AD L ^{11}
LD2: ^{145}LD R LL LE L ^{152}
LD3: ^{218}VE S LL DE L ^{225}
LD4: ^{267}LD E LM AS L ^{274}
LD5: ^{302}LD T ML GS L ^{309}

Figure 7. Structure of Paxillin.
Paxillin is composed of two major structural domains. They are the N-terminal LD (leucine-aspartate) motifs 1-5 (note their sequence identity above), and the C-terminal LIM (Lin-11, Isl-1, Mec-3) domains. Note the designated regions which are involved in binding to various proteins, such as FAK and vinculin. Adapted from Turner, 2000.

al., 1999; Herreros et al., 2000). Additionally, two of the LIM domains are responsible for targeting paxillin to FAs (Brown et al., 1996).

A LIM domain is composed of cysteine/histidine-rich, coupled zinc fingers, which together constitute a zinc-coordinating domain (Bach, 2000). Although they were originally thought to be DNA-interacting motifs, LIM domains are now known to function mainly as protein binding domains (Bach, 2000). Of the four 50-amino acid LIM domains present in the C-terminus of paxillin, research shows that an intact LIM3 is essential for targeting paxillin to FAs (Brown et al., 1996). Additionally, this same research demonstrates that a LIM2 double mutant decreases the efficiency of paxillin localization, which suggests that LIM2 might play a lesser but significant role in focal adhesion targeting (FAT). Supporting this supposition, it has been shown that during cell adhesion or growth factor stimulation, phosphorylation of the threonine and serine residues on LIM2 and LIM3, respectively, increases the localization of paxillin to FAs (Brown et al., 1998). Another study demonstrates that intact LIM3 and LIM4 domains are necessary for the binding of paxillin to the tyrosine phosphatase PTP-PEST at Pro 2, a novel proline-rich motif (Cote et al., 1999). The same research suggests that PTP-PEST contributes to the removal of paxillin from FAs and therefore facilitates FA turnover, this because the LIM3 domain of paxillin is involved in both FA targeting and tyrosine phosphatase binding.

Luecine-rich amino acid stretches with the general consensus sequence of LD X LL XX L are repeated five times within the N-terminus of paxillin (see Figure 7), and because of their conserved leucine (L) and aspartic acid (D) residues they have been named the LD motifs (Tumbarello et al., 2002). Through modeling, the LD motifs have

been predicted to form amphipathic, α-helical structures with their leucine residues being arranged on one face of the helix, resulting in a hydrophobic protein-binding surface (Tumbarello et al., 2002). LD motifs can be found in an extensive array of molecules ranging from structural proteins such as tensin (a FA protein) to regulatory proteins such as the guanine nucleotide-exchange factor Dbl (Brown et al., 1998). Because the LD motifs of paxillin are evenly spaced within the N-terminus, it has been theorized that they function together to recruit various signaling partners into close proximity to better facilitate signal transmission (Tumbarello et al., 2002). Multiple paxillin LD motifs have been found to bind the same protein; vinculin (a FA protein) binds to the LD1 (LDALLADL) motif, as well as to LD2 (LDRLLLEL) and LD4 (LDELMASL) (Turner, 2000). Conversely, an individual LD motif can have multiple binding partners; LD1 binds to both actopaxin and integrin-linked kinase (ILK) (Nikolopoulos and Turner, 2000; Nikolopoulos and Turner, 2001). Because of the similar characteristics of the paxillin LD motif binding partners, the theory that paxillin is involved with coordinating actin-cytoskeleton interactions has been reinforced (Turner, 2000). Interestingly, paxillin LD3 (VESLLDEL) has no known binding partners (Hoellerer et al., 2003).

Specific Aims

A better understanding of the etiology of NF2 needs to be acquired in order to prevent and/or reverse its effects. To achieve this goal, the mechanism of action of merlin's negative growth regulating function in SCs must be elucidated. A step in this

direction is to explore the molecular relationships between merlin and its various interactors within SCs.

Previous research conducted in our laboratory demonstrated that merlin and paxillin associate in SCs (Obremski et al., 1998). In order to determine the interaction type, direct binding assays were performed utilizing mixtures of various GST-merlin and GST-paxillin fusion proteins. The results of these assays demonstrated that the binding between recombinant merlin and paxillin occurs in a direct manner, *in vitro* (Fernandez-Valle et al., 2002). Additionally, it was shown that merlin interacts directly with paxillin through two discrete domains that our laboratory has designated as PBD1 and PBD2, for paxillin binding domain 1 and paxillin binding domain 2. Given these results, it would be of significance to determine which amino acid sequence(s) of paxillin bind to merlin.

Merlin associates with β1 integrins in SCs, and this has been demonstrated by both co-localization studies and by co-immunoprecipitation experiments (Obremski et al., 1998, Taylor et al., 2003). These discoveries, coupled with research showing that the membrane-proximal region of the β1 integrin cytoplasmic domain associates with paxillin (Schaller et al., 1995), lead to the question of whether merlin binds directly to β1 integrin or associates with β1 integrin through paxillin.

Merlin has been classified as an ERM family member based on a 49% overall homology to the other ERMs (Trofatter et al., 1993; Rouleau et al., 1993), and it has been shown to dimerize with its family member ezrin (Grönholm et al., 1999). Based on this data, and because merlin has been shown to bind directly to paxillin (Fernandez-Valle et al., 2002), it would be valuable to determine possible interactions between ezrin and paxillin.

Given the background information presented here, this thesis explores the molecular relationships between merlin and its various interactors within SCs. Therefore, the following questions will be addressed:

1. What amino acid sequence(s) of paxillin bind to merlin?
2. Does merlin bind directly to β1 integrin, or does it associate with β1 integrin through paxillin?
3. Do ezrin and paxillin associate with each other, and, if so, is the interaction direct or indirect?

MATERIALS AND METHODS

The following tables consist of lists of antibodies, reagents, and supplies that were utilized in the completion of this thesis. Vendor names are provided, as well as usage specifications.

Materials

Table 1. Primary Antibodies.

Antigen	Vendor	Host Species	Dilution/Use
$\beta 1\ Integrin_{cd}$	BD Biosciences	Mouse	1:100 / IB
T7	Cell Signaling	Mouse	1:2500 / IB
GST	Amersham Biosciences	Goat	1:1000 / IB
Merlin (C18)	Santa Cruz Biotechnologies	Rabbit	1:300 / IB
Merlin (A19)	Santa Cruz Biotechnologies	Rabbit	1:200 / IB
Paxillin	BD Biosciences	Mouse	1:10,000 / IB

IB: Immunoblot

Table 2. Secondary Antibodies.

Conjugate	Vendor	Host Species	Dilution/Use
Peroxidase	Jackson ImmunoReasearch	Goat	1:20,000 / IB
Peroxidase	Jackson ImmunoReasearch	Mouse	1:20,000 / IB
Peroxidase	Jackson ImmunoReasearch	Rabbit	1:20,000 / IB

IB: Immunoblot

Table 3. Additional Reagents and Supplies.

Product	Vendor	Use
LB medium	Bio 101, Inc.	Bacterial culturing
LB agar	Fisher Biotech	Bacterial culturing
Tryptone	Fisher Biotech	Bacterial culturing
Yeast	Fisher Biotech	Bacterial culturing
Ampicillin	Sigma	Bactericide
Kanamycin	Sigma	Bactericide
Isopropylthiogalactoside (IPTG)	Sigma	Protein induction
Aprotinin	Sigma	Protease inhibitor
Leupeptin	Sigma	Protease inhibitor
ALLN (calpain)	CalBiochem	Protease inhibitor
Sodium Pyrophosphate	Sigma	Protease inhibitor
Phenylmethanesulfonyl Fluoride (PMSF)	Sigma	Protease inhibitor
Sodium Fluoride (NaF)	Sigma	Protease inhibitor
Sodium Orthovandanate (SOV)	Sigma	Protease inhibitor
Complete EDTA-free PIC tablets	Roche	Protease inhibitor
PIC (EDTA free for His-tagged)	Sigma	Protease inhibitor
PIC (for GST-tagged)	Sigma	Protease inhibitor
Immobilon-P PVDF membrane	Millipore	Western Blot
Bovine Serum Albumin (BSA)	Sigma	Membrane blocking
SuperSignal Chemiluminescent Reagent	Pierce	Western Blot
GelCode Blue Stain Reagent	Pierce	Blue staining
Silver Stain Kit	BioRad	Silver staining
Tris-Acetate	Fisher Biotech	Buffer
Sodium Choride (NaCl)	MidWest	Buffer/general
Tris-HCl	Fisher Biotech	Buffer/SDS-PAGE
Bis-Acrylamide	BioRad	SDS-PAGE
Sodium dodecyl sulfate (SDS)	Amresco	Buffer/SDS-PAGE
Ammonium Persulfate (APS)	Amresco	SDS-PAGE
TEMED	BioRad	SDS-PAGE
Molecular Weight Markers	BioRad	SDS-PAGE
Agarose	Amresco	DNA gels
Hyperladder	Bioline	DNA marker
NP 40	Sigma	Buffer
Glycerol	Sigma	General
Triton X-100	Sigma	Protein purification
Lysozyme	Sigma	Protein purification
Benzonase Nuclease	Novagen	Protein purification
Imidazole	Sigma	Protein purification
BamHI	Invitrogen	Restriction digestion
EcoRI	Invitrogen	Restriction digestion
SmaI	Invitrogen	Restriction digestion
XhoI	Invitrogen	Restriction digestion
T4 DNA Ligase	Promega	DNA ligation
Shrimp Akaline Phosphotase (SAP)	USB Corp.	Cloning

Product	Vendor	Use
Cell culture dishes	Corning	Cell culture
Fetal Bovine Serum (FBS)	Hyclone	Cell culture
Forskolin	Sigma	Cell culture
Pituitary Extract (PEX)	Biomed. Tech	Cell culture
Dulbecco's Modified Eagle Medium (DMEM)	Life Tech.	Cell culture
Hanks Balanced Salt Solution	Life Tech.	Cell culture
Phosphate buffered saline (PBS)	Gibco	Cell culture
GST Bind/Wash Buffer	Novagen	Protein purification
GST Elution Buffer	Novagen	Protein purification
Glutathione Sepharose 4B Beads	Amersham	Protein purification
Ethanol	Sigma	General
Butanol	Sigma	Protein purification

Methods

Cell Culture

Frozen SCs, obtained from previous sciatic nerve dissections of newborn Sprague-Dawley rats (Charles River, Raleigh, NC) (Brockes et al., 1979), were thawed and then plated on PLL (200µg/ml)-coated tissue culture dishes. Cells were grown in DMEM containing 10% FBS, 20µg/ml PEX, and 2µM forskolin until used in experiments. Cells were passaged no more than six times.

Schwann Cell Protein Extraction

Medium was removed from the SC cultures, and then the cultures were rinsed twice with cold PBS. Cultures were incubated on ice in TAN buffer (10mM Tris-acetate pH 8, 100mM NaCl, 1%NP-40) containing protease and phosphatase inhibitors (20µg/ml

aprotinin, 10μg/ml luepeptin, 1mM SOV, 1mM sodium pyrophospate, 50mM NaF, 2mM PMSF) for 20 minutes (min). Cells were removed from the culture dish using a rubber policeman, and the solution was pipetted into a pre-chilled Eppendorf tube. The cell suspension was vortexed for 2 min, incubated for 15 min at 4°C while rotating, and was then centrifuged in an Eppendorf 5417C at 14,000rpm for 15 min at 4°C. The supernatant containing the protein lysate was removed and stored at -80°C until further use. The cellular debris pellet was also stored at -80°C until the completion of the experiment. Protein concentrations were determined for the lysate using the Bio-Rad D_C Protein assay (modified Lowry assay).

Electro-competent Bacteria Production

Electro-competent bacteria were produced for use in cloning. Three cultures of each the BL21 (expression), BL21(DE3) (expression), and XL1Blue (cloning) empty plasmids were prepared using 4ml of SOB medium (without Mg^{2+}, without antibiotics), and were incubated overnight (~ 16 hrs) at 37°C. The cultures were expanded to 50ml, and grown until an optical density (OD) reading of 0.4 to 0.5. The cultures were then aliquoted into pre-chilled tubes and centrifuged at 5000rpm for 10 min at 4°C. The supernatant was discarded, and the pellets were resuspended in 25ml of sterilized, ice-cold 10% glycerol. The cultures were centrifuged at 5000rpm for 15 min at 4°C and the supernatant was immediately removed. The glycerol wash step was repeated an additional time, and the supernatant was removed. The remaining bacterial slurry for

each plasmid was aliquoted (40µl) into pre-chilled micro-centrifuge tubes and then flash-frozen in a dry ice/ethanol bath. These were then stored at -80°C.

The competent bacteria were tested by electroporation to determine if they had been washed enough; they had. An aliquot of cells was transformed with pGEX-6P as a positive control. Samples of the competent bacteria were plated on agar containing antibiotics and incubated overnight at 37°C. The three competent bacterial strains showed no colony growth, as they shouldn't, because they had no plasmids and therefore no antibiotic resistance. The positive control colony did show growth, as it should because the pGEX plasmid confers ampicillin resistance. Colony growth verified that the electro-competent bacteria were acceptable.

Generation of His-Merlin Constructs

His-merlin-N term (NT) and His-merlin-C term (CT) glycerol stocks were available from earlier research conducted in our laboratory. Sub-cloning was necessary to generate the additional two His-tagged merlin constructs required for this thesis research.

Cultures of 30ml LB broth and ampicillin (30µl) were begun using either BL21, XL1-Blue, or DH5α strains of bacterial glycerol stocks containing plasmids with the insert sequences merlin-NTΔPBD1 (merlin without the PBD1 sequence) and merlin-CTΔPBD2 (merlin without PBD2). Following overnight incubation, the plasmids were purified from the bacterial cultures using the QIAGEN Plasmid Purification Midi Kit. The resulting plasmid DNA was resuspended in 150µl of milli-pore water (mp), and OD

readings were performed in order to determine the amount of each plasmid DNA obtained.

Digestion reactions were set up to cut each insert from its plasmid DNA using BamHI (5µl) and EcoRI (5µl) restriction enzymes (REs). The 25µg-plasmid DNA reaction mixtures were digested overnight in a 37°C liquid incubator. In order to separate each insert DNA from its plasmid DNA, the digestion mixtures were run on a 1% agarose gel. Additionally, a sample of the pre-cut and de-phosphorylated pET-28a(+) plasmid was run to verify that it had been previously cut. Using an ultraviolet (UV) light, the size of each insert DNA was confirmed.

The merlin inserts were purified out of the gel using the QIAquick Gel Extraction Kit, and then OD readings were performed to determine the DNA amounts obtained. Ligation mixtures, consisting of 30 femto-moles (f-mol) of each DNA, were set up using T4 Ligase to anneal each merlin insert into its pET vector. The reaction mixtures were incubated overnight in a 16°C liquid bath. Following incubation, the DNA was precipitated out of solution using 1-butanol followed by ethanol, and was then re-suspended in mp water (10µl).

Each insert-containing plasmid (1µl) was used in the transformation of both XL1Blue and BL21DE3 electro-competent bacteria. The bacteria were transformed using the Gene Pulser (200Ω, 25µF, 1.80V), were incubated in SOC medium for 1 hr, and were then spread (30 to 50µl) onto warm agar plates. The agar plates contained kanamycin (50µl/ml) for the selection of positive clones, and the plates were incubated overnight at 37°C.

Following incubation, 5ml LB broth cultures containing kanamycin (final conc. of 50µl/ml) were begun using colonies picked from both the XL1Blue and BL21DE3 agar plates. These cultures were incubated overnight at 37°C, and the following day 3ml of each culture was purified for plasmid using the QIAprep Spin Miniprep Kit. Each plasmid was then digested with both EcoRI and BamHI restriction enzymes, and the digestions were run on a 1% agarose gel to confirm presence of the inserts. As seen in Figure 8, construction of positive clones was confirmed. Finally, gycerol stocks were prepared and stored at -80°C for each bacterial culture containing the positive clones.

Binding Assays

Affinity Pull-down Assay (Indirect Binding)

SCs were grown to confluency and the total protein was extracted, as previously described. GST and GST-paxillin fusion proteins (0.5µg) were immobilized onto 50µl (bed volume) of Glutathione Sepharose 4B beads. The beads were brought up to 1ml with TAN extraction buffer, and were then incubated for 30min with rocking at RT. Following incubation, the samples were centrifuged at 500g for 5 min and the supernatant was removed. SC lysate, 200µg, was added to the immobilized GST-paxillin fusion proteins. The samples were incubated O/N at 4°C while rocking. Following incubation, the beads were centrifuged at 500g for 5 min at 4°C, and then were rinsed 2 times with

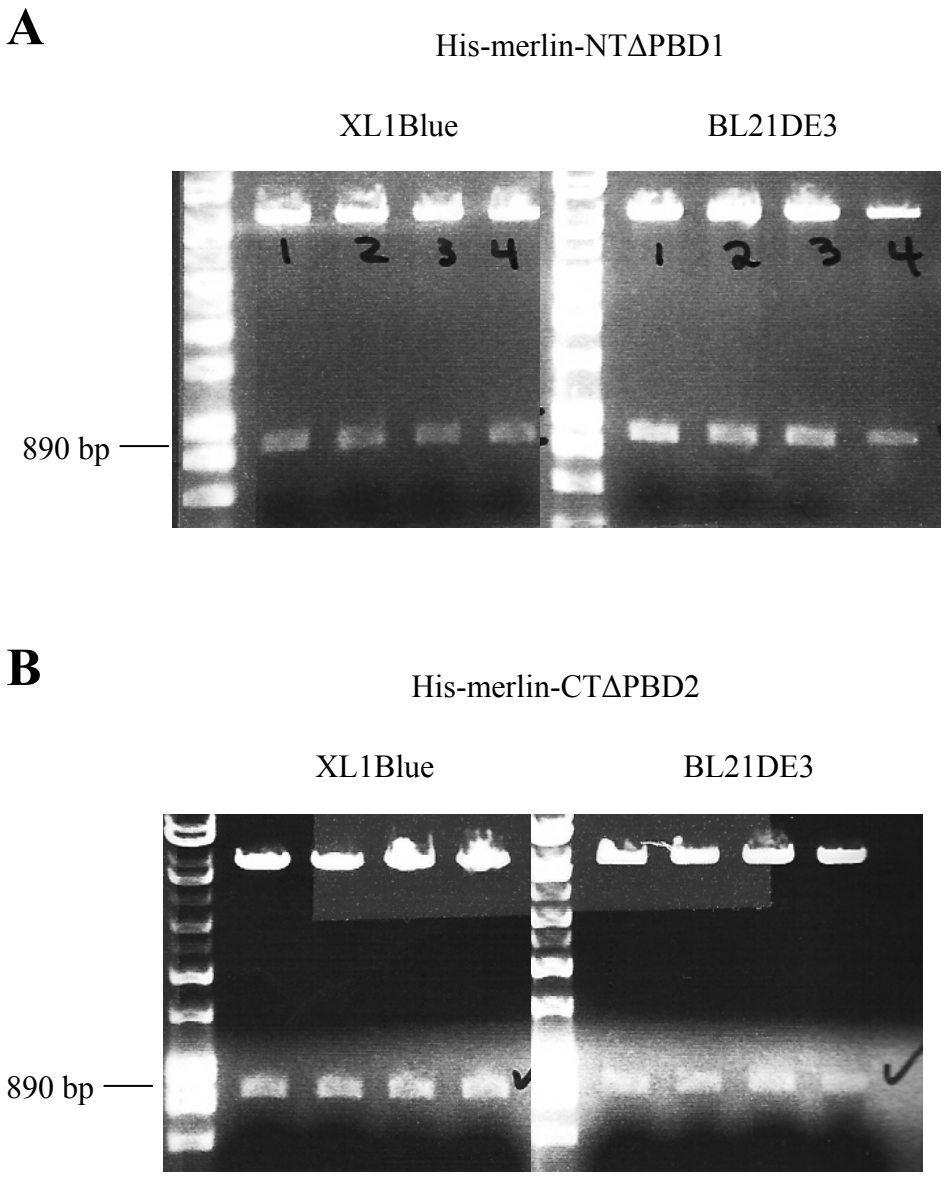

Figure 8. Confirmation of Positive His-Merlin Clones.
The transformed bacteria were plated on agar and incubated overnight at 37°C. Overnight cultures were set up with bacterial colonies picked from the agar plates for each merlin insert, and these were incubated overnight at 37°C. Plasmid DNA was purified from the cultures, the plasmids were digested with BamHI and EcoRI restriction enzymes, and the digestion solutions were resolved on a 1% agarose gel to confirm the presence of the merlin-NΔPBD1 and -CΔPBD2 inserts. His-merlin-NTΔPBD1 insert presence was confirmed in 4 clones of each XL1Blue and BL21DE3 at the approximated size of 890 bp (A). His-merlin-CTΔPBD2 insert presence was confirmed in 4 clones of each XL1Blue and BL21DE3 at the approximated size of 890 bp (B).

1X GST Bind/Wash Buffer containing 0.1% TX-100. Following the rinses, the beads were resuspended in 40µl of 3X SDS sample buffer, and were boiled at 100°C for 10 min. Western blot analysis then followed.

Direct Binding Assays

In general, the various GST-tagged fusion proteins (0.25µg) were immobilized onto 20µl (bed volume) of Glutathione Sepharose 4B beads. The beads were brought up to 1ml with 1X PBS containing 0.1% TX-100, and were then incubated for at least 2 hr at 4°C while rocking. Following incubation, the samples were centrifuged at 500g for 5 min at 4°C, and the supernatant was removed and saved. The beads were rinsed 2 times with 1X PBS containing 0.1% TX-100; the rinse fractions were saved. The various His-tagged fusion proteins (0.25µg) were then added to the beads, and the buffer (1X PBS containing 0.1% TX-100 and 500mM NaCl) was brought up to 1ml. The samples were incubated O/N at 4°C while rocking. Following incubation, the beads were centrifuged at 500g for 5 min at 4°C, and the supernatant was removed and saved. The samples were rinsed 3 times with 1X PBS containing 0.1% TX-100 and 500mM NaCl. Following the rinses, the beads were resuspended in 40µl of 5X SDS sample buffer, and were boiled at 100°C for 10 min. Western blot analysis then followed.

Western Blot Analysis

Protein samples, which had already been resuspended in SDS Sample buffer, were boiled for 3 min at 100°C to ensure denaturization, and were then resolved by sodium dodecyl sufate-polyacrylamide gel electrophoresis (SDS-PAGE). The smaller recombinant proteins were run on 12% gels for better seperation, while the larger recombinant proteins were run on either 8% or 10% gels. Immediately following SDS-PAGE, the proteins were electroblotted onto PVDF membranes. Membranes were stained with India ink that was diluted 1:1000 in TBS-T. Membranes were then blocked for 1hr at RT in either 5% powdered milk in TBS-T (blocking buffer) or in TBS-T alone depending on the primary antibody used. Membranes were then incubated with the indicated primary antibodies diluted in the appropriate blocking buffer on a surf blot apparatus for 1hr at RT. After rinsing multiple times in TBS-T, the membranes were incubated with the indicated HRP-conjugated secondary antibodies for 30 min at RT. Membranes were exposed to SuperSignal Chemiluminescent reagents. Detection of proteins was performed using Kodak X-ray film placed over the membranes for various exposure times, and the film was developed in an automated film developer.

RESULTS

Recombinant Protein Expression and Purification

GST-Paxillin Fusion Proteins

The GST-paxillin-full length (FL), GST-paxillin-N term (NT), and GST-paxillin-C term (CT) fusion proteins were generated from the pGEX-6P plasmid. The GST-paxillin-LD fusion proteins were generated from bacterial colonies transformed with the pGEX-2TK plasmid received as a gift from Dr. C. Turner of SUNY Upstate Medical University in Syracuse, New York. The pGEX plasmid was used to confer a glutathione S-transferase (GST) tag onto the N-terminus of the recombinant protein produced from the bacterial cultures.

Starting with 4ml of LB broth, cultures were begun using previously prepared glycerol stocks of transformed BL21 bacteria containing each construct of interest. Ampicillin was added (final concentration of 100μg/ml) to the cultures in order to select for transformed bacteria. The cultures were incubated at 37°C, overnight, with shaking at 300rpm for aeration. Following incubation, the bacterial cultures were expanded by adding 2YT broth to a 30ml final volume; again, ampicillin was added (30μl). The bacterial cultures were grown until an OD reading of 0.6 to 0.8 was reached. Recombinant protein expression was induced using IPTG (final concentration of 1 mM).

The bacterial cultures were then incubated at 30 to 37°C for between 2 to 6 hrs with shaking at 250 rpm for aeration. The ranges given for induction temperature and time are dependant upon the specific paxillin construct. Following incubation, the bacteria were pelleted at 6000rcf for 20 min at 4°C. The supernatant was removed, and each pellet was either immediately utilized or stored at -80°C until use.

If previously frozen, the bacterial pellets were thawed on ice. Each pellet was resuspended in 1ml of GST lysis buffer (10mM Tris-HCl, pH 8.0, 100µl PIC, 1% TX-100). Lysozyme (1mg/30ml pellet) was added and the suspension was incubated for 15 min on ice. Bacterial lysis was obtained either by French press (2 times at 700psi) or by sonication (3 times at 10 sec each time followed by 30 sec pauses). The resulting lysate was centrifuged at 14,000rpm for 20 min at 4°C. The supernatants containing the recombinant proteins were transferred to pre-chilled Eppendorf tubes, and were either used immediately or stored at -20°C.

Purification of the recombinant GST-tagged paxillin proteins was done in batch using Glutathione Sepharose 4B beads (50µl bed volume/sample), which were rinsed 2 times with 1X PBS prior to use. The beads were added to the lysates, and the samples were incubated overnight at 4°C while rotating. Following incubation, the samples were centrifuged at 500g for 5 min, and the supernatant was removed and stored. To remove remaining impurities, the beads were rinsed 3 times in 1X GST Bind/Wash Buffer. Following the final rinse, the beads were resuspended in 200µl of 1X GST Elution Buffer (50mM Tris-HCl, 10mM reduced glutathione) with 0.1% TX-100. To elute the purified proteins from the beads, the samples were incubated at 4°C while rotating. After 30 min,

the samples were centrifuged at 510g for 5 min at 4°C and the supernatants containing the purified recombinant proteins were collected.

Protein concentrations were determined using either the modified Lowry assay or the Bio-Rad Protein Assay (modified Bradford assay). The recombinant proteins were resolved using SDS-PAGE, and were Blue Stained to verify their presence and to determine their relative purity. Figure 9 shows the expressed and purified GST-paxillin LD fusion proteins.

His-Paxillin Fusion Proteins

The His-paxillin-full length (FL) fusion protein was generated from the pET-28a(+) plasmid, which confers a His tag to the N-terminus of the recombinant protein produced. Starting with 5ml of LB broth, the culture was begun using a previously prepared glycerol stock of BL21DE3 bacteria. Kanamycin was added (final concentration of 50μg/ml) to the culture to select for transformed bacteria. The culture was incubated at 37°C overnight, with shaking at 300rpm for aeration. Following incubation, the culture was expanded by adding LB broth to a 30ml final volume; again, kanamycin was added (30μl). The culture was grown until an OD reading of 0.6 to 0.8 was reached. Recombinant protein expression was induced using IPTG (final concentration of 1mM). The culture was incubated at 32°C for 4 hrs with shaking at 250rpm for aeration. Following incubation, the bacteria were pelleted at 6000rcf for 20 min at 4°C. The supernatant was removed, and the pellet was stored at -80°C until use.

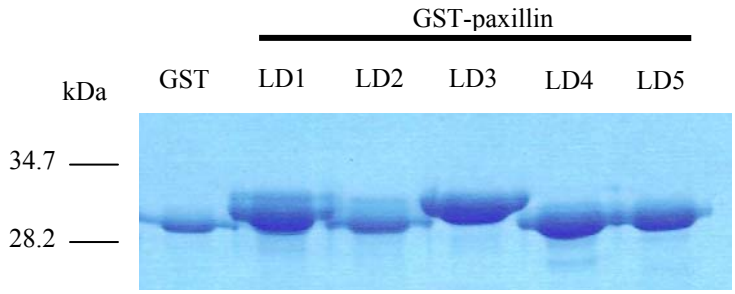

Figure 9. Expression and Purification of GST-Paxillin Fusion Proteins.
Overnight bacterial cultures were expanded until an OD of 0.6 to 0.8, and then expression was induced with 1mM IPTG for 4 hrs at 30°C in the presence of ampicillin. Pelleted bacteria were lysed by sonication and purified in batch using Glutathione Sepharose 4B beads. Proteins were eluted with 1X GST Elution Buffer in 200µl aliquots. Protein concentration was determined by the modified Lowry assay. The recombinant proteins were resolved by SDS-PAGE (12%), and then Blue Stained to determine their relative purity.

The frozen pellet was thawed on ice, and then resuspended in 5ml of bind buffer (0.02M sodium phosphate, 0.5M NaCl, pH 7.4). Lysozyme (1mg/ml) was added and the solution was incubated on ice for 30 min, followed by sonication. Benzonase (1µl) was added and the solution was incubated for an additional 30 min on ice. The solution was centrifuged at 14,000rpm for 20 min at 4°C, and the supernatant was saved as the crude lysate.

The His-paxillin-FL fusion proteins were purified using the Amersham Biosciences HiTrap Chelating HP column, charged with 0.1M $NiSO_4$ in distilled water, according to the manufacturer's instructions. Briefly, the chelating column was washed with distilled water, charged with the $NiSO_4$ solution, washed again with water, and then equilibrated with bind buffer. Immediately prior to application, the crude lysate was passed through a 0.45µm PES filter for clarification. The lysate was applied to the column with a syringe, and the column was rinsed with bind buffer containing 5mM of imidazole. The proteins were eluted from the column, in one step, using elution buffer (0.02M sodium phosphate, 0.5M NaCl, 0.5M imidazole, pH 7.4).

The concentration was determined using the Bradford assay, and the purified protein was resolved using SDS-PAGE. The gel was then Blue Stained to verify the presence of His-paxillin and to determine its relative purity. Figure 10 shows the two purified elutions of the His-paxillin fusion protein.

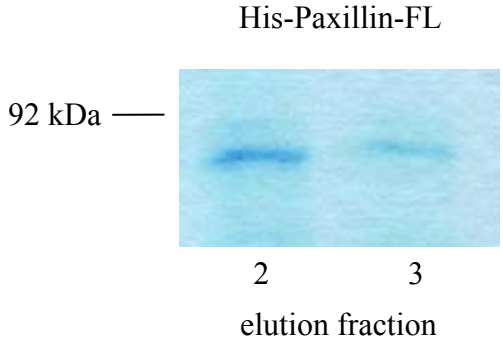

Figure 10. Expression and Purification of the His-Paxillin Fusion Protein. Overnight bacterial cultures were expanded until an OD of 0.6 to 0.8. Bacterial expression of the recombinant protein was induced with 1mM IPTG for 4 hrs at 32°C in the presence of kanamycin. Pelleted bacteria were lysed by sonication and purified using Amersham Biosciences HiTrap Chelating HP columns charged with 0.1M NiSO4. Proteins were eluted with 0.02M sodium phosphate, 0.5M NaCl, 0.5M imidazole, pH 7.4, and protein concentration was determined by the Bradford assay. The recombinant proteins were resolved by SDS-PAGE (10%), and then Blue Stained to determine their relative purity.

His-Merlin Fusion Proteins

Expression of the merlin constructs was begun with 4ml of LB broth, to which was added the transformed bacteria containing each construct of interest and kanamycin (final concentration of 50μg/ml). The cultures were incubated at 37°C, overnight, with shaking at 300rpm for aeration. Following incubation, the bacterial cultures were expanded by adding LB broth to a 30ml final volume; again, kanamycin was added (30μl). The bacterial cultures were grown until an OD reading of 0.6 to 0.8 was reached. Recombinant protein expression was induced using IPTG (final concentration of 1 mM). The bacterial cultures were then incubated at 33°C for 4 hrs with shaking at 250rpm for aeration. Following incubation, the bacteria were pelleted at 6000rcf for 20 min at 4°C. The supernatant was removed, and each pellet was either immediately utilized or stored at -80°C until use.

If previously frozen, the bacterial pellets were thawed on ice. The His-tagged merlin constructs were purified using the QIAGEN Ni-NTA Spin Kit according to the manufacturer's instructions. Briefly, each pellet was resuspended in lml of lysis buffer (50mM NaH_2PO_4, 300mM NaCl, 10mM imidazole, pH 8.0). Lysozyme (1mg/30ml pellet) was added and the suspension was incubated for 30 min on ice. During incubation, one tablet of Complete EDTA-free PIC (protease inhibitor cocktail) was added to the suspension. Bacterial lysis was obtained by sonication, and the resulting lysate was centrifuged at 14,000rpm for 20 to 30 min at 4°C. The supernatants containing the recombinant proteins were transferred to pre-chilled Eppendorf tubes, and were either used immediately or stored at -20°C. The Ni-NTA spin columns were

equilibrated with lysis buffer, and the cleared lysates were added to the columns. The spin columns were centrifuged for 2 to 4 min at 700g, followed by collection of the flow-through. The spin columns were washed 4 times with wash buffer (50mM NaH_2PO_4, 300mM NaCl, 20mM imidazole, pH 8.0) to remove non-specific proteins. The His-tagged merlin proteins were then eluted off the columns 3 times using elution buffer (50 mM NaH_2PO_4, 300mM NaCl, 250mM imidazole, pH 8.0). The purified recombinant proteins were collected in 200µl aliquots, and the protein concentrations were determined using the Bradford assay. The recombinant proteins were resolved using SDS-PAGE, and were immuno-blotted to verify their presence and to determine their relative purity. Figure 11 displays the purified merlin fusion proteins.

GST-Ezrin Fusion Proteins

The ezrin recombinant proteins were prepared from ezrin cDNAs received as a gift from Dr. O. Carpén of the University of Helsinki in Finland. The ezrin-NT (1-309) insert was received in the pGEX-4T-1 plasmid; the restriction enzymes used in its cloning were EcoRI and (BamHI, SmaI, and SalI). The ezrin-CT insert was received in the pGEX-4T-3 plasmid, and its restriction enzyme sites were SmaI and XhoI.

Each cDNA (1µl) was used to transform both XL1Blue and BL21 electro-competent bacteria. The bacteria were transformed using the Gene Pulser (200Ω, 25µF, 1.80V), and were incubated in SOC medium for 1 hr. The cultures were spread (50µl) onto warm agar plates containing ampicillin (100µg/ml) for the selection of positive clones, and the plates were incubated overnight at 37°C.

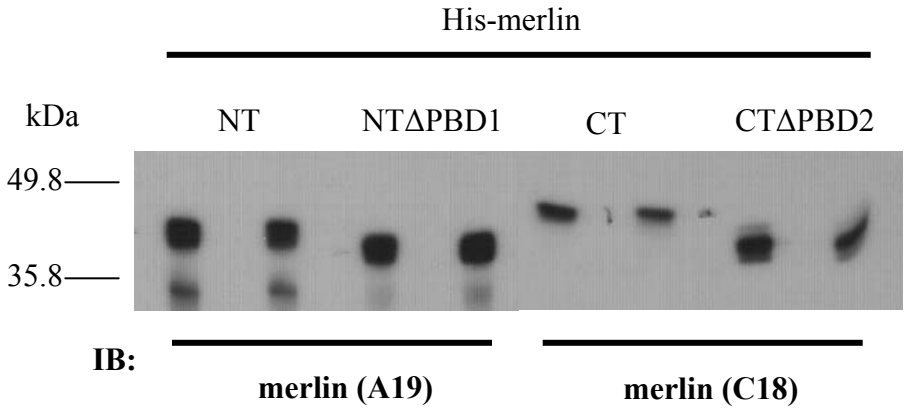

Figure 11. Expression and Purification of the His-Merlin Fusion Proteins. Overnight bacterial cultures were expanded until an OD of 0.6 to 0.8. Bacterial expression of the recombinant proteins was induced with 1mM IPTG for 4 hrs at 32°C in the presence of kanamycin. Pelleted bacteria were lysed by sonication and purified using the QIAGEN Ni-NTA Spin Kit. Proteins were eluted with 50mM NaH2PO4, 300mM NaCl, 250mM imidazole, pH 8.0, and protein concentration was determined by the Bradford assay. The recombinant proteins were resolved by SDS-PAGE (12%), and were analyzed by Western Blot to determine their relative purity.

Starting with 4ml of LB broth and ampicillin (final concentration of 100µg/ml), cultures were begun using colonies picked from the BL21 agar plates containing each insert of interest. The cultures were incubated at 37°C, overnight, with shaking at 300 rpm for aeration. Following incubation, the bacterial cultures were expanded by adding 2YT broth to a 50ml final volume; again, ampicillin was added (50µl). The bacterial cultures were grown until an OD reading of 0.6 to 0.8 was obtained. Protein expression was induced using IPTG (final concentration of 1mM), and the bacterial cultures were incubated at 35°C for 5 hrs with shaking at 250rpm for aeration. Following incubation, the bacteria were pelleted at 6000rcf for 20 min at 4°C. The supernatant was removed, and each pellet was either immediately utilized or stored at -80°C until use.

If previously frozen, the bacterial pellets were thawed on ice. Each pellet was resuspended in 3.5ml of GST lysis buffer (10mM Tris-HCl, pH 8.0, 100µl PIC, 1% TX-100, 2mM PMSF). Lysozyme (1mg/30ml pellet) was added and the suspension was incubated for 30 min on ice. Bacterial lysis was obtained by sonication (3 times at 10 sec each time followed by 30 sec pauses). The resulting lysate was centrifuged at 14,000 rpm for 20 min at 4°C. The supernatants containing the recombinant proteins were transferred to pre-chilled Eppendorf tubes, and were either used immediately or stored at -20°C.

Purification of the GST-tagged ezrin fusion proteins was completed, in batch, using Glutathione Sepharose 4B beads (50µl bed volume/sample), which were rinsed 2 times with 1X PBS prior to use. The beads were added to the lysates, and the samples were incubated 1.5 hrs at 4°C while rotating. Following incubation, the samples were centrifuged at 500g for 5 min, and the supernatant was removed and stored. To remove

remaining impurities, the beads were rinsed 3 times in 1X GST Bind/Wash Buffer. Following the final rinse, the beads were resuspended in 200µl of 1X GST Elution Buffer (50mM Tris-HCl, 10mM reduced glutathione) with 0.1% TX-100, and the samples were incubated at 4°C while rotating. After 30 min, the samples were centrifuged at 510g for 5 min at 4°C and the supernatants containing the purified recombinant proteins were collected.

Protein concentrations were determined using the Bradford assay. The recombinant proteins were resolved using SDS-PAGE, and were Blue Stained to verify their presence and to determine their relative purity (Figure 12).

GST-β1 Integrin Cytoplasmic Domain (CD) Fusion Proteins

The GST-β1 integrin CD (GST-$\beta1_{cd}$) fusion protein was generated from the pGEX-2TK plasmid. Starting with 5ml of LB broth, the culture was begun using a previously prepared glycerol stock of transformed BL21 bacteria containing the insert of interest. Ampicillin was added (final concentration of 100µg/ml) to the culture in order to select for transformed bacteria. The culture was incubated at 37°C, overnight, with shaking at 300rpm for aeration. Following incubation, the bacterial culture was expanded by adding 2YT broth to a 45ml final volume; again, ampicillin was added (45µl). The culture was grown until an OD reading of 0.6 to 0.8 was reached, and recombinant protein expression was induced using IPTG (final concentration of 1mM). The culture was then incubated at 30°C for 4 hrs with shaking at 250rpm for aeration. Following

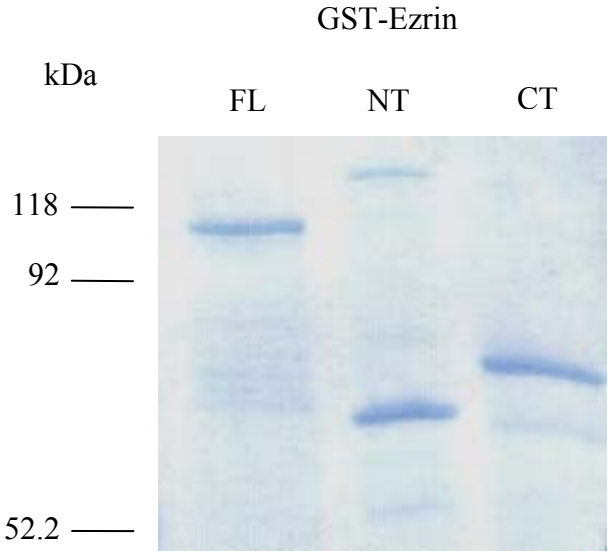

Figure 12. Expression and Purification of GST-Ezrin Fusion Proteins.
cDNA (1µl) for each construct was used to transform BL21 and XL1Blue bacteria using electroporation, and the transformed bacteria were plated on agar containing ampicillin (100µg/µl) and incubated overnight at 37°C. Overnight cultures were set up with bacterial colonies picked from the agar plates for each ezrin construct, and these were incubated overnight at 37°C. Overnight bacterial cultures were expanded until an OD of 0.6 to 0.8, and bacterial expression of the recombinant proteins was induced with 1mM IPTG for 5 hrs at 35°C in the presence of ampicillin. Pelleted bacteria were lysed by sonication and purified in batch using Glutathione Sepharose 4B beads. Proteins were eluted with 1X GST Elution Buffer in 200µl aliquots. Protein concentrations were determined by the Bradford assay. The recombinant proteins were resolved by SDS-PAGE (10%), and then Blue Stained to determine their relative purity.

incubation, the bacteria were pelleted at 6000rcf for 20 min at 4°C. The supernatant was removed, and each pellet was either immediately utilized or stored at -80°C until use.

If previously frozen, the bacterial pellets were thawed on ice. Each pellet was resuspended in 1.25ml of lysis buffer (20mM Tris-HCl, pH 8.0, 300mM NaCl, 1% TX-100, 100µl PIC, 1mM Na pyrophosphate, 50mM NaF, 1mM SOV, 2mM PMSF). Lysozyme (1mg/30ml pellet) was added and the suspension was incubated for 30 min on ice. Bacterial lysis was obtained by sonication (3 times at 10 sec each time followed by 30 sec pauses), and the resulting lysates were centrifuged at 14,000rpm for 15 min at 4°C. The supernatants containing the recombinant proteins were transferred to pre-chilled Eppendorf tubes, and were either used immediately or stored at -80°C.

Purification of the GST-$\beta 1_{cd}$ fusion protein was completed utilizing Amersham Biosciences Glutathione Sepharose 4B Microspin columns. Briefly, the columns were vortexed to resuspend the resin, and were centrifuged to remove the storage buffer. The lysates (600µl) were added to the columns and the samples were rocked at room temperature (RT) for 10 min. Following incubation, the samples were centrifuged at 735g for 1 min, and the supernatant was removed and stored. To remove remaining impurities, the columns were rinsed 3 times with 1X PBS containing 0.1% TX-100. The recombinant protein was eluted from the columns 2 times in 200µl of Glutathione Elution Buffer (50mM Tris-HCl, 10mM reduced glutathione) with 0.1% TX-100. Each elution was incubated for 15 min at 4°C while rocking, and the columns were centrifuged at 735g for 1min at 4°C to collect the eluates. The GST-$\beta 1_{cd}$ fusion protein concentrations were determined using the Bradford assay. The recombinant proteins were resolved

using SDS-PAGE, and the gel was Blue Stained, as seen in Figure 13, to verify the presence of the proteins and to determine the relative purity.

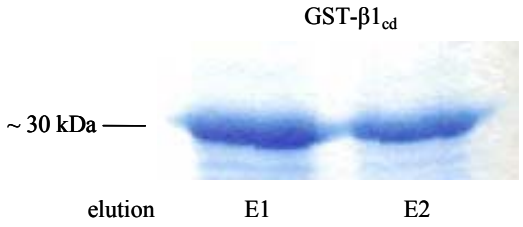

Figure 13. Expression and Purification of the GST-β1cd Fusion Proteins. Overnight bacterial cultures were expanded until an OD of 0.6 to 0.8. Bacterial expression of the recombinant protein was induced with 1mM IPTG for 4 hrs at 30°C in the presence of ampicillin. Pelleted bacteria were lysed by sonication and purified using Amersham Biosciences Glutathione Sepharose 4B Microspin columns. Proteins were eluted with 1X GST Elution Buffer in 200µl aliquots. Protein concentration was determined by the Bradford assay. The recombinant proteins were resolved by SDS-PAGE (12%), and then Blue Stained to determine their relative purity.

Binding Assays

Merlin–Paxillin Interactions

Affinity Pull-down Assay (Indirect Binding)

Previous studies conducted in this laboratory demonstrate that merlin and paxillin bind in a direct manner, *in vitro* (Fernandez-Valle et al., 2002). Subsequent research revealed that merlin interacts with paxillin through two discrete domains designated as PBD1 and PBD2, for paxillin binding domain 1 and paxillin binding domain 2 (Fernandez-Valle et al., 2002). It follows that the binding site(s) for merlin on the paxillin protein should be identified. The first experiment conducted toward this end was an affinity pull-down assay. Various GST-paxillin fusion proteins were produced as described previously. The paxillin fusion proteins were immobilized onto Glutathione Sepharose beads and were then mixed with confluent SC lysate, obtained as described in the Materials and Methods section. Following incubation and rinsing, the samples were analyzed by Western blot utilizing merlin and GST antibodies.

As seen in the total extract (TE) lane of Figure 14, endogenous merlin migrates at ~ 68 kDa when detected with merlin antibody; this lane was used as a reference for merlin presence in the binding assays. Merlin was detected in both the GST-pax-FL and GST-pax-NT lanes, indicating that endogenous merlin is able to bind both full-length paxillin and the N-terminus of paxillin, *in vitro*. An additional band of approximately 48 kDa was detected in both the GST- pax-FL and GST-pax-NT lanes as well. Previous

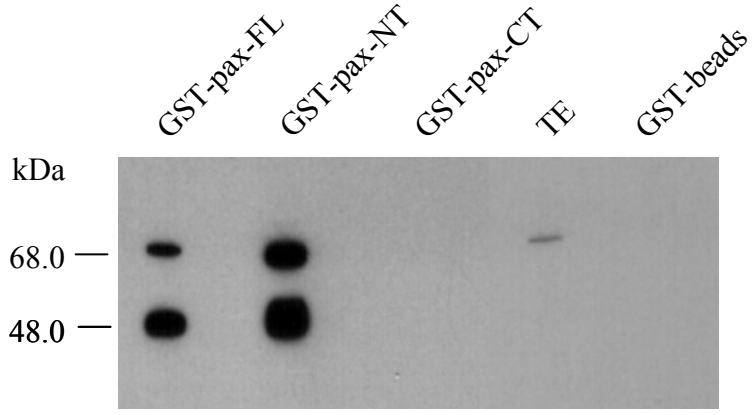

IB: merlin (C18)

Figure 14. GST-Paxillin Full-Length and N-Terminus Bind to Merlin From Confluent Schwann Cell Lysate.
SCs were grown to confluency and the total protein was extracted. GST and GST-paxillin fusion proteins (0.5μg), immobilized on glutathione sepharose beads, were incubated with 200μg of SC lysate. The samples were resolved by SDS-PAGE (10%) and then immunoblotted with rabbit anti-merlin antibody (C18). The bands present at 68kDa in the GST-pax-FL and GST-pax-NT lanes indicate that merlin binds to full length paxillin as well as the N-terminus of paxillin, *in vitro*. The 48kDa bands detected in the GST-pax-FL and GST-pax-NT lanes are most likely merlin cleavage products. Total extract (TE) serves as a positive control verifying the presence and molecular weigh of the endogenous merlin in the SC lysate.

research has shown that when utilizing the merlin C18 antibody in Western blot analysis of SC lysates, up to four bands (120, 88, 68, and 48 kDa) of merlin can be detected (Chen et al., 2000), with the 68 kDa band being regarded as the wild-type (Shaw et al., 1998b). The faster migrating 48 kDa band is most likely a cleavage product of merlin, as studies have shown that calpain cleaves merlin and therefore results in numerous cleavage products which can be detected by the C18 antibody (Kimura et al., 2000). The 48 kDa band was not detected in the TE lane, indicating a relatively lower abundance of merlin cleavage products in the SC extract as compared to that of the total protein. No merlin was detected in the GST-pax-CT lane, suggesting that merlin does not bind to the C-terminus of paxillin, *in vitro*. Additionally, merlin was not detected in the GST-beads control lane, indicating that merlin binding to the paxillin fusion proteins was not the result of non-specific binding to either the GST-tag or the beads themselves.

Direct Binding Assays

The results of the previous experiment suggested that binding interactions between merlin and paxillin should be focused on just the N-terminus of paxillin. To determine which paxillin amino acid residues directly facilitate the merlin-paxillin interaction, direct binding assays were conducted between the N-terminal GST-paxillin LD fusion proteins and the His-tagged merlin fusion proteins. The paxillin and merlin fusion proteins were produced as described previously. The GST-paxillin fusion proteins were immobilized onto Glutathione Sepharose beads, and then the His-tagged merlin

fusion proteins were added to the buffer. Following incubation and rinsing, the samples were analyzed by Western blot using merlin and GST antibodies.

Figure 15A shows that merlin was detected (via the A19 antibody) in the GST-pax-LD3 lane, indicating that the N-terminus of merlin binds to the paxillin LD3motif, *in vitro*. Additionally, merlin was detected in the GST-pax-LD4 and -LD5 lanes, indicating that the N-terminus of merlin also binds to paxillin LD4 and LD5, but to a lesser extent. As revealed in Figure 16A, when utilizing the C18 antibody, merlin was differentially detected as binding to paxillin LD motifs 2 through 5. Specifically, the C-terminus of merlin exhibited strong binding to paxillin domains LD2 and LD3, *in vitro*. Merlin was also detected in the GST-pax-LD4 and -LD5 lanes. This indicates that, as with the N-terminus, the C-terminus of merlin binds paxillin LD4 and LD5, but with a weaker affinity than with domains LD2 and LD3. Neither of the merlin fusion proteins were detected in the GST-pax-LD1 lane, suggesting that merlin does not bind to paxillin LD1, *in vitro*. Additionally, no merlin was detected in either of the GST-beads or beads-alone control lanes, indicating that merlin binding to the recombinant paxillin proteins was not the result of non-specific binding to either the GST-tag or the beads themselves. To demonstrate equal loading of the GST-paxillin fusion proteins, the membranes were stripped and re-blotted with the GST antibody. Figures 15B and 16B demonstrate equal loading for each paxillin LD fusion protein present in each binding assay.

The results from the previous experiments conducted for this thesis suggested that, due to its interactions with both the amino and carboxy termini of merlin, the paxillin LD3 motif is an integral factor in merlin-paxillin binding interactions.

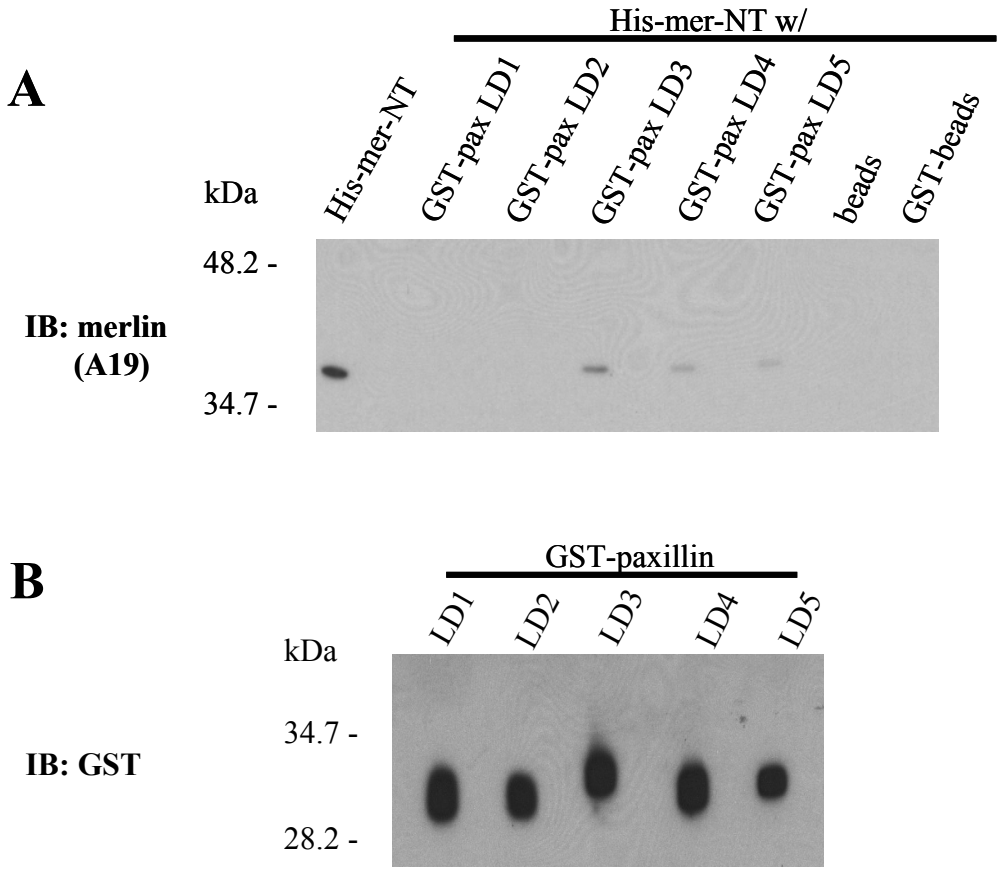

Figure 15. GST-Paxillin-LD3 Binds Directly to His-Merlin N-Terminus.
GST and GST-paxillin fusion proteins (0.25µg), immobilized on glutathione sepharose beads, were incubated with His-merlin N term fusion proteins (0.25µg). The samples were resolved by SDS-PAGE (12%), and Western blot analyses were performed utilizing rabbit anti-merlin antibodies. Recombinant His-mer-NT was run to verify its molecular weight as detected by the merlin A19 antibody. The band present in the GST-pax-LD3 lane indicates that the merlin N-terminus binds directly to paxillin at LD domain 3, *in vitro*. Weaker binding was detected at LD domains 4 and 5 (A). Following the initial blotting, the membrane was stripped and re-probed with goat anti-GST to show equal loading of the GST-paxillin fusion proteins (B).

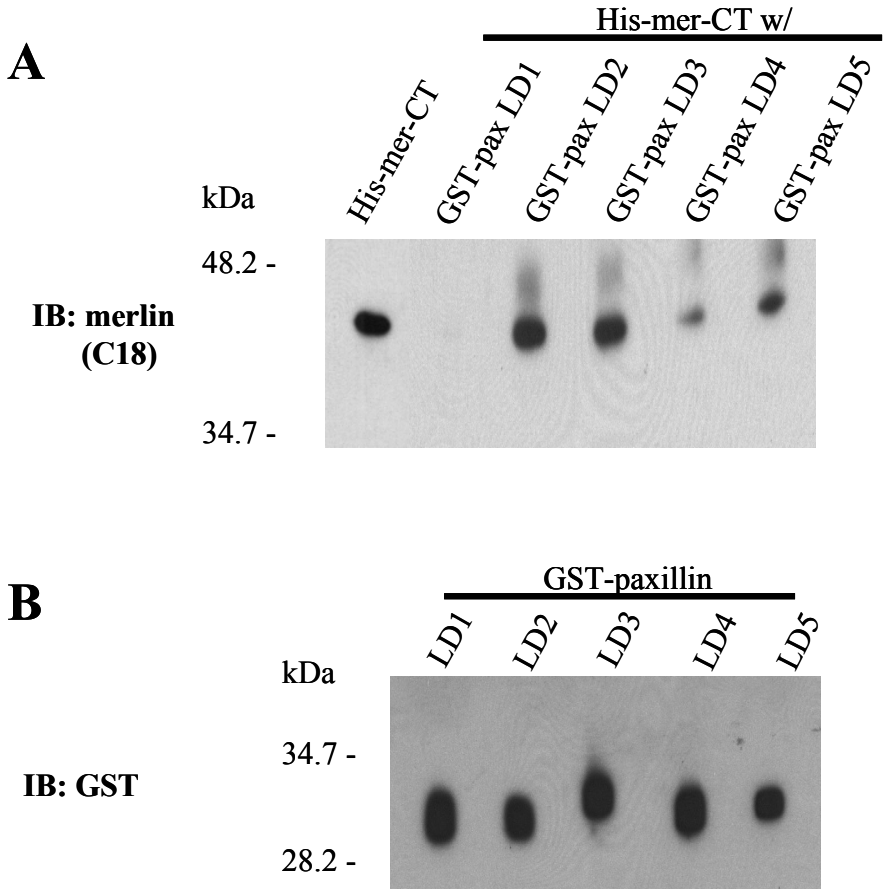

Figure 16. GST-Paxillin-LDs 2 and 3, Predominantly, Bind Directly to His-Merlin C-Terminus.

GST-paxillin fusion proteins (0.25μg), immobilized on glutathione sepharose beads, were incubated with His-merlin C term fusion proteins (0.25μg). The samples were resolved by SDS-PAGE (12%), and Western blot analyses were performed utilizing rabbit anti-merlin antibodies. Recombinant His-mer-CT was run to verify its molecular weight as detected by the merlin C18 antibody. The bands present in the GST-pax -LD2 and -LD3 lanes indicate that the merlin C-terminus binds directly and predominantly to paxillin at LD domains 2 and 3, *in vitro*. Weaker binding was detected at LD domains 4 and 5 (A). Following the initial blotting, the membrane was stripped and re-probed with goat anti-GST to demonstrate equal loading of the GST-paxillin fusion proteins (B).

Additionally, previous studies conducted in this laboratory have shown that the merlin PBD1 domain binds directly with paxillin. Taken together, these results suggest that the paxillin LD3 and merlin PBD1 sequences are essential for direct binding between paxillin and merlin. To determine the validity of this hypothesis, a final and specific direct binding assay was conducted. Recombinant His-tagged merlin lacking the PBD1 sequence, His-mer-NTΔPBD1, was produced as described previously. The GST-pax-LD3 fusion proteins were immobilized onto Glutathione Sepharose beads, and then both of the His-mer-NT and His-mer-NTΔPBD1 fusion proteins were added to the buffer solutions. Following incubation and rinsing, the samples were analyzed by Western blot utilizing merlin and GST antibodies.

The first and second lanes of Figure 17 exhibit the apparent molecular weights of the recombinant proteins His-mer-NT and His-mer-NTΔPBD1, respectively, and were used as references for this binding assay. The results show that the N-terminus of merlin was detected in the GST-pax-LD3 lane, but that the merlin N-terminus minus the PBD1 sequence was not. These results confirm that, *in vitro*, paxillin LD3 binds directly to the merlin N-terminus, and that specifically, the binding occurs directly between the paxillin LD3 motif and the merlin PBD1 domain. This conclusion is supported by the result which demonstrates that deletion of the merlin PBD1 sequence abrogates binding to the paxillin LD3 domain. The results of these experiments are significant in that, to date, there are no published reports documenting the identification of binding partners for the paxillin LD3 motif (Hoellerer et al., 2003).

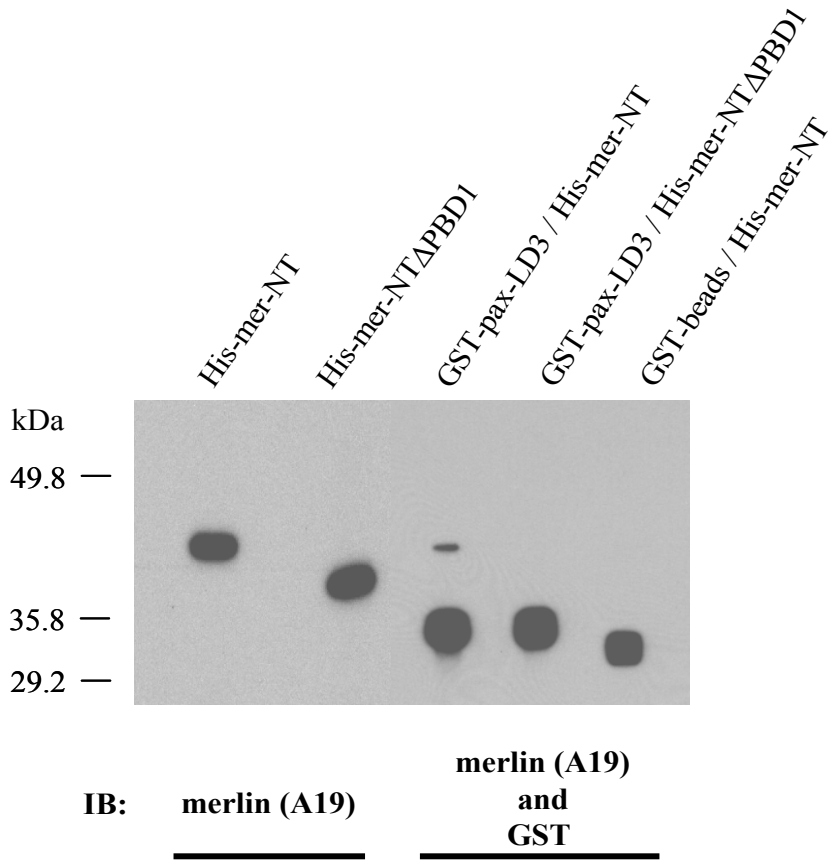

Figure 17. GST-Paxillin LD3 Binds Directly to His-Merlin N Term, but Not to His-Merlin N Term Lacking the PBD1 Domain.
GST-paxillin LD3 fusion proteins (0.25µg), immobilized on glutathione sepharose beads, were incubated with the His-merlin N term and His-merlin N term lacking the PBD1 domain (0.25µg) fusion proteins. The proteins were resolved by SDS-PAGE (12%), and Western blot analyses were performed using rabbit anti-merlin A19 and goat anti-GST antibodies. His-mer-NT and His-mer-NTΔPBD1 were run to verify their molecular weights as detected by the merlin A19 antibody. The upper band present in the GST-pax LD3 / His-mer-NT lane indicates that the merlin N-terminus binds directly to paxillin at LD domain 3, *in vitro*. The lower band in this same lane verifies the presence of the GST-pax-LD3 fusion protein as detected by the GST antibody. The absence of a band corresponding to the molecular weight of the His-mer-NTΔPBD1 in the GST-pax LD3 / His-mer-NTΔPBD1 lane indicates that the deletion of PBD1 abrogates merlin binding to paxillin. The band detected in this same lane verifies the presence of the GST-pax-LD3 in the assay. As a negative control, the absence of a band corresponding to the molecular weight of the His-mer-NT in the GST-beads / His-mer-NT lane demonstrates that the recombinant His proteins do not bind to the GST tag non-specifically.

Merlin-β1 Integrin Interactions

Schaller et al. has demonstrated that the membrane-proximal region of the β1 integrin cytoplasmic domain associates with paxillin (Schaller et al., 1995), and merlin and β1 integrin have been shown to associate in SCs (Obremski et al., 1998; Taylor et al., 2003). Additionally, merlin and paxillin have been shown to bind in a direct manner (Fernandez-Valle et al., 2002). Based on these observations, it is of significance to determine whether merlin directly binds to the cytoplasmic domain of β1 integrin.

In the first experiment of this series, direct binding assays were conducted between the GST-β1 integrin cytoplasmic domain (cd) and both the His-merlin fusion proteins (mer1: merlin isoform 1, and mer2: merlin isoform 2) and the His-paxillin fusion protein. All recombinant proteins were produced as described previously. The GST-$\beta1_{cd}$ fusion proteins were immobilized onto Glutathione Sepharose beads, and the His-mer1, -mer2, and -pax fusion proteins were added separately to the buffer of each of the GST-$\beta1_{cd}$ samples. Following incubation and rinsing, the samples were analyzed by Western blot using merlin, T7, and GST antibodies. Figure 18A shows the results of the binding assays between the GST-$\beta1_{cd}$ and the His-merlin and His-paxillin fusion proteins, while Figure 18B demonstrates equal loading of the GST-$\beta1_{cd}$ fusion protein. As seen in Figure 18A, all three of the His-tagged fusion proteins exhibited binding to GST-$\beta1_{cd}$. The fact that binding was also exhibited in the negative control lanes (GST-beads and GST) as well, suggested that the binding and rinsing buffer compositions were not stringent enough to disallow non-specific binding. This finding led to additional experiments (results not shown) in which both the bind and rinse buffer stringencies were adjusted

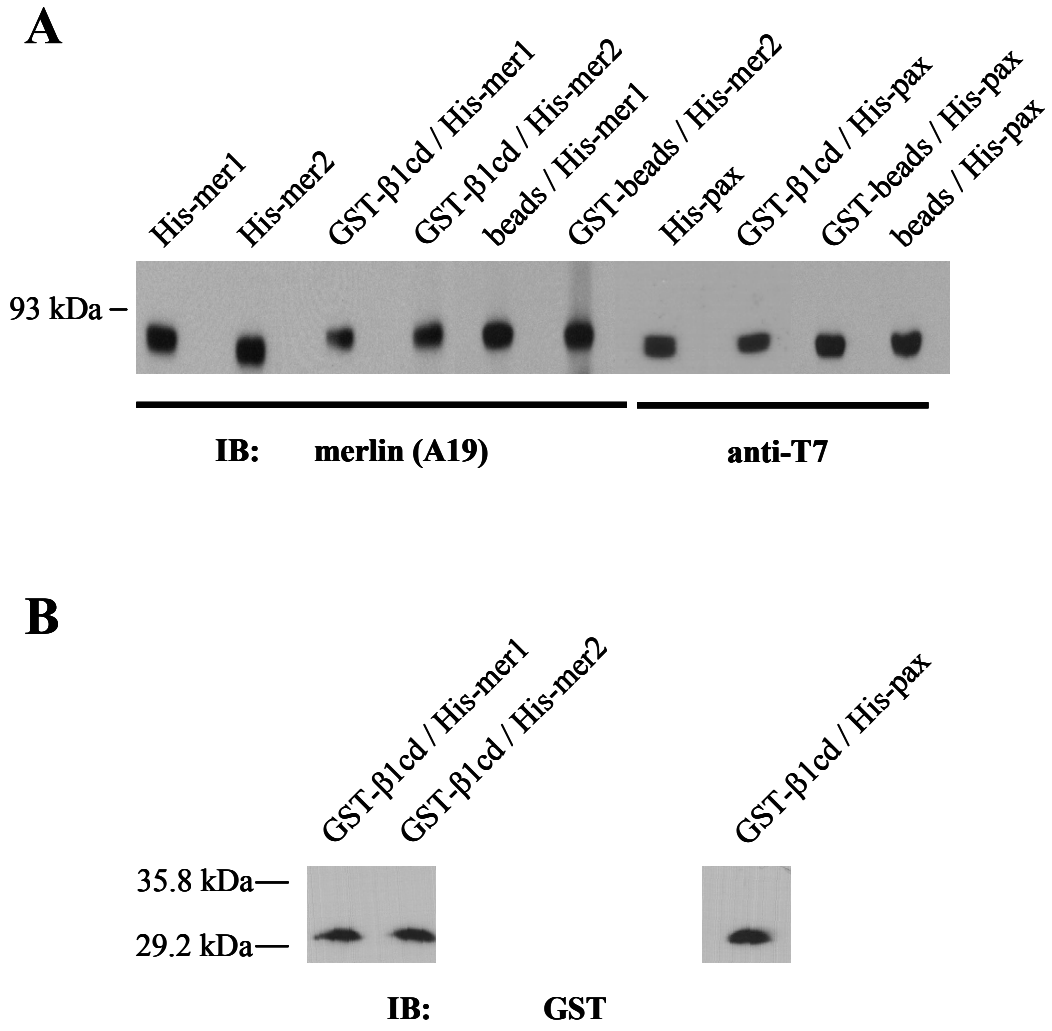

Figure 18. GST-β1 Integrin Cytoplasmic Domain Binds Directly to His-Merlin 1, His-Merlin 2, and His-Paxillin.
The GST-β1cd fusion protein (3.0ng), immobilized on glutathione sepharose beads, was incubated with His-merlin1, His-merlin2, and His-paxillin (1.0ng) fusion proteins. The proteins were resolved by SDS-PAGE (8%), and Western blot analyses were performed using the rabbit anti-merlin A19 and T7 antibodies. The His-mer1, His-mer2, and His-pax recombinant proteins were run alone to demonstrate their apparent molecular weights. The results indicate that the His-mer1, His-mer2, and His-pax fusion proteins bound to GST-β1cd, as well as did all of the negative controls, suggesting a high degree of non-specific binding (A). Following the initial blotting, the membrane was stripped and re-probed with goat anti-GST to demonstrate equal loading of the GST-β1cd fusion protein (B).

for each set of proteins. Optimal buffer conditions were unable to be determined (in the time given) for the binding assay between GST-$\beta 1_{cd}$ and His-paxillin, therefore this line of research was set aside.

Buffer stringencies were determined for the assay between the $\beta 1_{cd}$ and merlin fusion proteins, and it was decided to limit the assay to merlin isoform 1, versus both isoforms 1 and 2. Therefore, the next experiment focused on the binding interactions between GST-$\beta 1_{cd}$ and the His-merlin N- (His-mer-NT) and C-termini (His-mer-CT) fusion proteins. Recombinant proteins were produced as described previously. GST-$\beta 1_{cd}$ proteins were immobilized onto Glutathione Sepharose beads, and the His-mer-NT and His-mer-CT fusion proteins were added separately to each sample. Following incubation and extensive rinsing, the samples were analyzed by Western blot using merlin and GST antibodies. Figure 19A shows that the C terminus of merlin was detected in the GST-$\beta 1_{cd}$ lane. This result indicates that direct binding occurs, *in vitro*, between the cytoplasmic domain of β1 integrin and the merlin C-terminus. No merlin was detected in the beads / His-mer-CT control lane. This result supports the validity of the binding shown between the merlin C-terminus and the cytoplasmic domain of β1 integrin indicating that this binding is not the result of non-specific interactions. As the Western blot analyses show in Figure 19A, the merlin N-terminus was not detected in the GST-$\beta 1_{cd}$ / His-mer-NT lane. This result appears to indicate that no binding occurred between the N-terminus of merlin and the cytoplasmic domain of β1 integrin. But when the membrane was reprobed with the anti-GST antibody in order to verify the presence

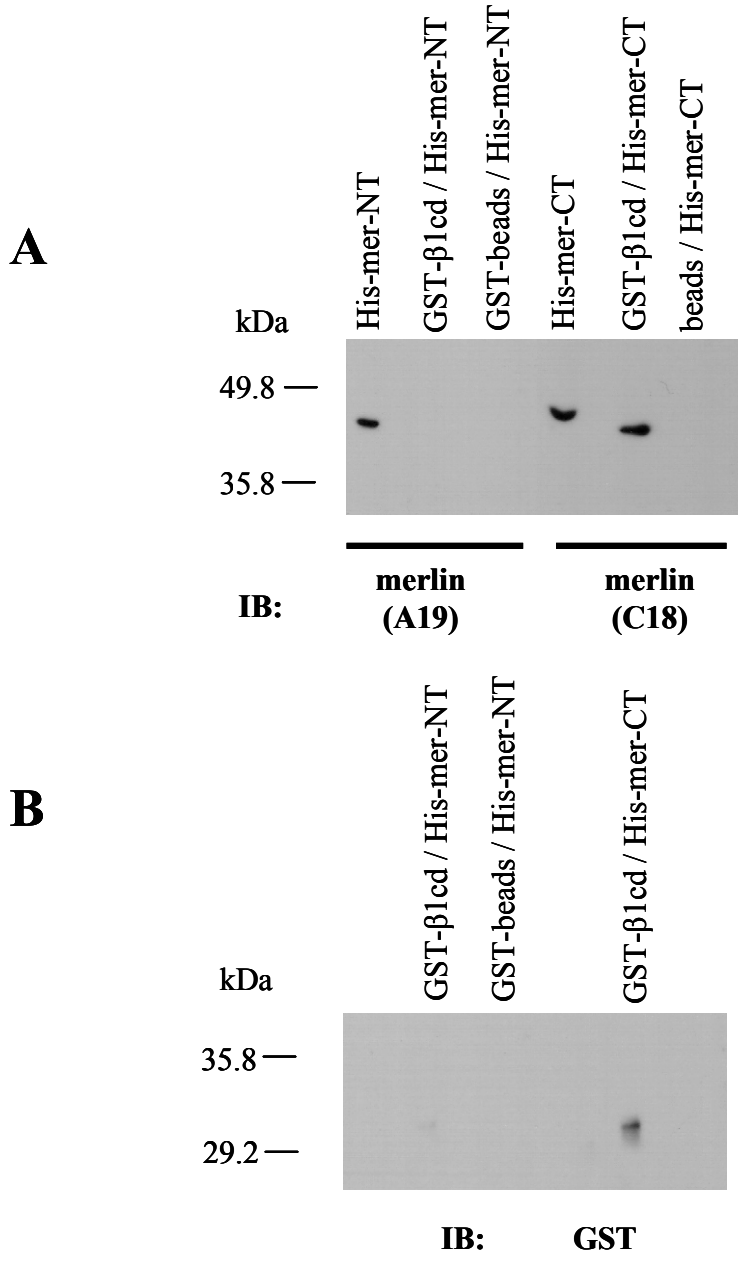

Figure 19. The GST-β1 Cytoplasmic Domain Binds Directly to the C-Terminus of Merlin.

GST-β1cd fusion proteins (3.0ng), immobilized on glutathione sepharose beads, were incubated with the recombinant proteins His-mer-NT and His-mer-CT (1.0ng). The proteins were resolved by SDS-PAGE (12%), and Western blot analyses were performed using rabbit anti-merlin A19 and C18 antibodies. The His-mer-NT and His-mer-CT fusion proteins were run alone to demonstrate their apparent molecular weights. The results indicate that the C-terminus of merlin binds to the cytoplasmic domain of β1 integrin, *in vitro* (A). Following the initial blotting, the membrane was stripped and re-probed with goat anti-GST for equal loading purposes (B).

of GST-$\beta 1_{cd}$ within the binding assay, recombinant GST-$\beta 1_{cd}$ was only weakly detected in the GST-$\beta 1_{cd}$ / His-mer-NT lane (Figure 19B). This data provides inconclusive evidence as to the interactions between these two fusion proteins, as there may not have been enough GST-$\beta 1_{cd}$ present on the beads to facilitate binding between them and the His-mer-NT protein. Additionally, as seen in Figure 19B, no GST was detected in the GST-beads / His-mer-NT control lane, as there should be. These results suggest that perhaps a contaminant of some type was introduced into the purified batch of His-mer-NT recombinant protein which caused the dissociation of the recombinant proteins from the beads. Additional research should be conducted in order to determine whether or not the merlin N-terminus binds to the cytoplasmic domain of β1 integrin.

Paxillin-Ezrin Interactions

Merlin, an ERM family protein, has been shown to dimerize with its ERM family member ezrin, both *in vitro* and *in vivo* (Grönholm et al., 1999). This interaction, coupled with the demonstration of direct binding between merlin and paxillin, suggests that paxillin-ezrin interactions should be investigated. Direct binding assays were conducted between the His-paxillin and the GST-ezrin fusion proteins. Both the paxillin and ezrin recombinant proteins were produced as described previously. The GST-ezrin fusion proteins were immobilized onto Glutathione Sepharose beads, and His-paxillin was added to each sample. Because of previous difficulties in determining the optimal buffer conditions when using His-paxillin fusion proteins in a direct binding assay, this experiment was set up, in parallel, utilizing both low-salt (137mM) and high-salt

(500mM) buffer conditions. Following incubation and extensive rinsing under both sets of buffer conditions, the samples were analyzed by Western blot using T7 and GST antibodies. As seen in Figure 20A, under the low-salt conditions, paxillin was detected strongly in the GST-ez-NT lane. Additionally, paxillin was detected, although much weaker, in the ezrin full-length and C-terminus lanes, as well as in the beads-alone control lane. Because paxillin was also detected in the negative control lane (beads / His-paxillin) the results of all binding detected under the low-salt conditions should be interpreted as non-specific. Figure 20B displays the results of the parallel binding assay conducted utilizing high-salt buffers, and Figure 20C demonstrates equal loading of the GST-ezrin proteins. Under high-salt buffer conditions, paxillin was detected in the GST-ez-NT lane, indicating that, *in vitro*, paxillin binds directly to the N-terminus of ezrin. In support of this result, no paxillin was detected in either of the negative control lanes (beads / His-paxillin and GST-beads / His-paxillin), indicating that the paxillin-ezrin binding was specific.

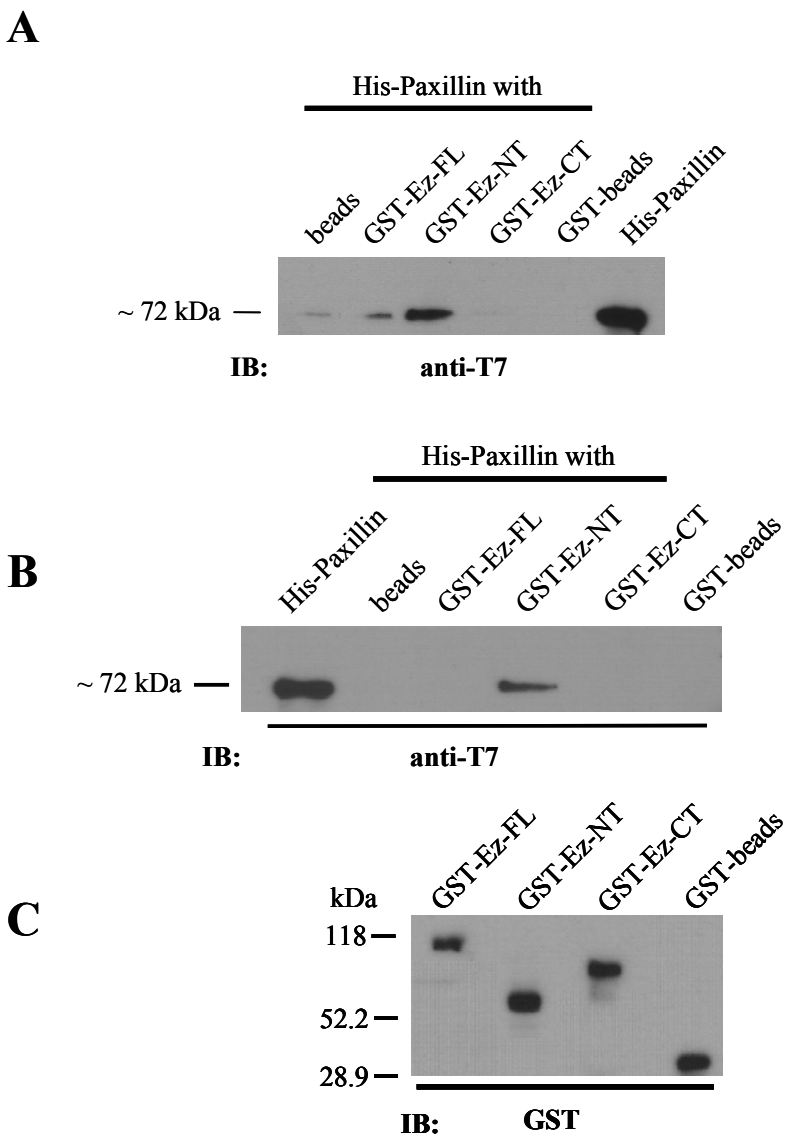

Figure 20. His-Paxillin-FL Binds to the Ezrin-N-Terminus Under High Salt Buffer Conditions.
GST-ezrin fusion proteins (0.5µg) were immobilized onto 20µl (bed volume) of Glutathione Sepharose beads, and His-paxillin(0.5µg) was added to each sample. The samples were incubated and rinsed with 1X Tris-HCl containing 0.1% TX-100 with either 137mM or 500mM NaCl. The proteins were resolved by SDS-PAGE (10%), and Western blot analyses were performed using mouse anti-T7 antibody. The results indicate that under low salt buffer conditions, binding of GST-ez-FL, -NT, and CT occurs with His-paxillin. The binding between these proteins is non-specific as binding of His-paxillin to the negative control (beads-alone) also occurs (A). Under high salt (500mM) buffer conditions, the results indicate that the N-terminus of ezrin binds to paxillin, *in vitro* (B). Following initial blotting, the membrane was stripped and reprobed with goat anti-GST for equal loading purposes (C).

DISCUSSION

Although it is well established that merlin functions as a tumor suppressor, its biological mechanism of action as it functions as a tumor suppressor has yet to be completely determined. The goal of this thesis was to examine the molecular relationships between merlin and a few of its various interactors within the signal transduction pathways of SCs. The results of this investigation will serve to further illuminate merlin's tumor suppressor function mechanism of action in SCs. The major findings of this thesis research are as follows:

1. The paxillin LD3 motif mediates merlin-paxillin interactions, *in vitro*, by binding directly to the merlin PBD1 domain,
2. The cytoplasmic domain of β1 integrin binds directly to the merlin C-terminus, *in vitro*, and
3. Paxillin binds directly to the N-terminus of ezrin, *in vitro*.

Merlin-Paxillin Interactions

As stated previously, research conducted in this laboratory has demonstrated that merlin interacts with paxillin in a direct manner through two separate and specific sequences within the merlin molecule termed PBD1 and PBD2, for paxillin binding domain 1 and 2, respectively (Fernandez-Valle et al., 2002). For the purpose of determining which paxillin amino acid sequence(s) aids in facilitating the merlin-paxillin interactions, a series of binding assays was conducted. The data obtained from the first of these experiments suggest that the N-terminus of paxillin is instrumental in mediating merlin-paxillin interactions. Further experiments, which demonstrate that LD3 binds to the merlin N-terminus and that LD's 2 and 3 bind to the merlin C-terminus, illustrate that multiple paxillin LD motifs play an important role in the binding of paxillin to both the N- and C-termini of merlin. The results revealing that more than one paxillin LD motif binds to merlin is consistent with previous research. FAK has been shown to bind to both the LD2 and LD4 domains of paxillin, while vinculin has been shown to bind the LD1, LD2, and LD4 motifs (Brown et al., 1996; Turner et al., 1999).

Paxillin LD3 is an integral factor in the binding between merlin and paxillin, as is suggested by the results which reveal that LD3 interacts with both the amino and carboxy termini of merlin. Reinforcing this supposition, the final merlin-paxillin binding results presented here demonstrate that the paxillin LD3 motif interacts directly and specifically with the merlin PBD1 domain, *in vitro*. From this result, it can be interpreted that both the paxillin LD3 and merlin PBD1 sequences are crucial for mediating merlin-paxillin binding. This conclusion is supported by the result which demonstrates that deletion of

the merlin PBD1 sequence abrogates binding to the paxillin LD3 motif. The finding that paxillin LD3 specifically mediates direct binding to merlin PBD1 fleshes out the model of merlin-paxillin interactions in SCs proposed by our laboratory (Fernandez-Valle et al., 2002). Briefly stated, it is specifically the LD3 domain of paxillin, through its binding to merlin at PBD1, which positions merlin at the plasma membrane where it can interact with various signaling proteins. Figure 21 illustrates the direct interaction between merlin and paxillin.

The discovery of a binding partner to the paxillin LD3 motif is of some significance in and of itself as, to date, there are no published reports documenting the identification of binding partners for the paxillin LD3 motif (Brown & Turner, 2004).

Merlin-β1 Integrin Interactions

Studies show that merlin co-immunoprecipitates and co-localizes with β1 integrin in SCs (Obremski et al., 1998; Taylor et al., 2003). More recently, research has revealed that merlin and paxillin bind each other directly (Fernandez-Valle et al., 2002). Additionally, our laboratory has shown that merlin is recruited into a β1 integrin complex at the plasma membrane. The results of these studies raised the question of whether merlin binds directly to β1 integrin or associates with β1 integrin through paxillin. To determine the answer to this question, direct binding assays were performed between merlin and the β1 integrin cytoplasmic domain. The assay results indicate that the cytoplasmic domain of β1 integrin binds directly to the C terminus of merlin, *in vitro*.

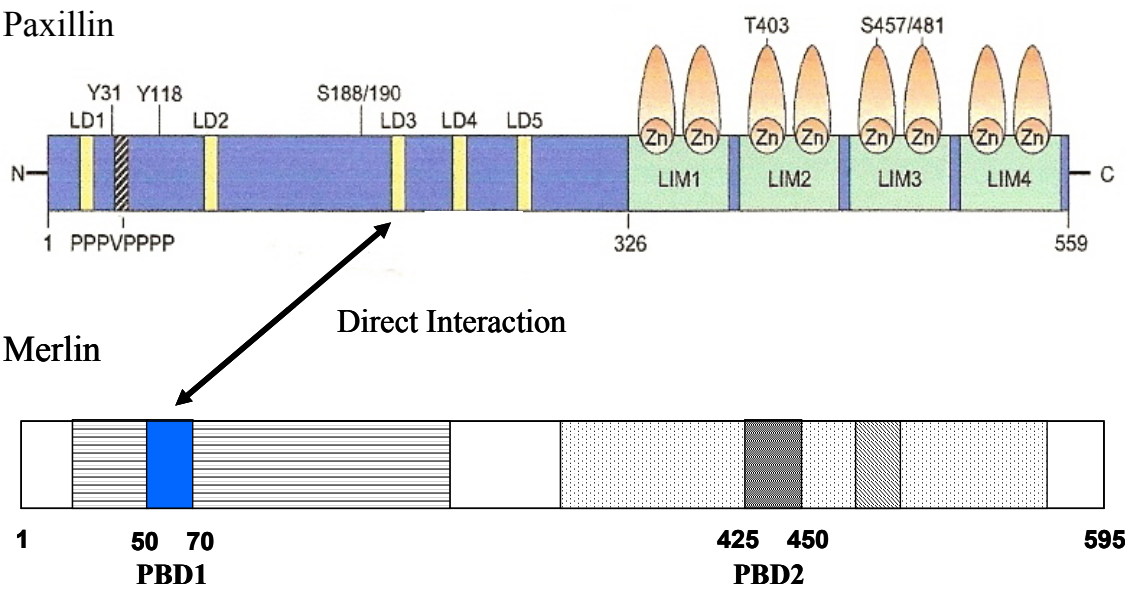

Figure 21. The 1st Direct Binding Partner for the Paxillin LD3 Domain Has Been Identified as the Merlin PBD1 Domain.
The paxillin LD3 motif binds directly to the PBD1 domain of merlin, *in vitro*. This conclusion is supported by results which demonstrate that the deletion of the merlin PBD1 sequence abrogates binding to the paxillin LD3 domain.

This conclusion is consistent with research which shows that talin, a FERM family protein like merlin, binds directly to β1A, a β1 integrin cytoplasmic domain splice variant (Pfaff et al., 1998). Additional studies reveal that the C-terminal rod of talin can bind to the cytoplasmic domains of both β1 and β3 integrins (Martel et al., 2000; Xing et al., 2001).

Based on the results presented in this thesis, coupled with the current research sited, one could theorize that merlin, in it's open and inactive conformation (in terms of tumor suppressor function), is shuttled to the plasma membrane by paxillin LD3 for the purpose of binding to the cytoplasmic domain of β1 integrin in order to transmit growth permissive signals. Figure 22 illustrates the proposed binding interactions between merlin, paxillin, and β1 integrin.

Interestingly, it had been proposed that there are two integrin binding sites per talin molecule (Knezevic et al., 1996). This supposition has since been proven true. In addition to its C-terminus binding to β integrins, studies have revealed that the N-terminal FERM domain of talin is able to bind to the membrane-proximal region of β integrin cytoplasmic tails (Calderwood et al., 1999; Patil et al., 1999). Because it has been shown that there are both N- and C-terminal integrin binding domains on talin, it has been suggested that the globular head and rod-like tail domains of talin participate in cooperative binding to integrins (Yan et al., 2001). Based on this information, future studies should be conducted to determine whether the N-terminus of merlin also binds to the cytoplasmic domain of β1 integrins.

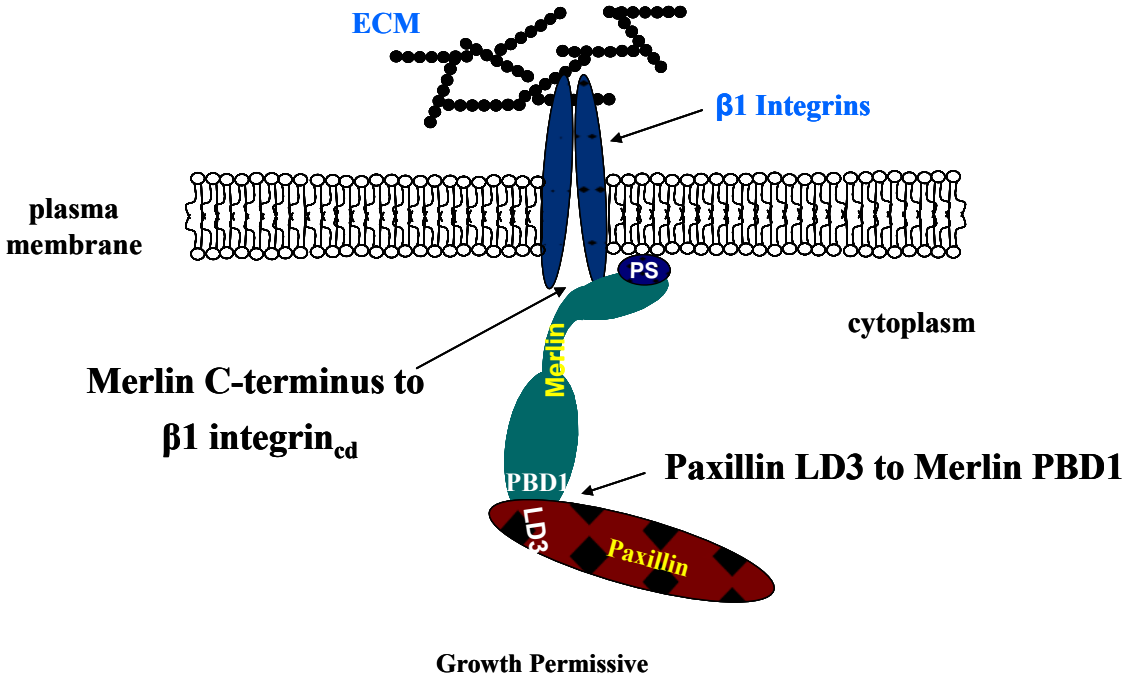

Figure 22. Merlin/Paxillin/β1 Integrin Binding Model.
Merlin, in its open and inactive conformation (in terms of its tumor suppressor function), is shuttled to the plasma membrane, via the paxillin LD3 motif binding to the PBD1 domain, for the purpose of binding to the cytoplasmic domain of β1 integrin in order to propagate growth permissive signals.

Paxillin-Ezrin Interactions

Merlin and ezrin, both ERM family members, have demonstrated the ability to undergo both homo- and heterodimerization, *in vitro* and *in vivo* (Grönholm et al., 1999). These data, taken into consideration with this laboratory's previous findings showing that the merlin N-terminus binds directly with paxillin (Fernandez-Valle et al., 2002), suggested that the interactions between ezrin and paxillin be examined. To determine possible ezrin-paxillin interactions, direct binding assays were conducted between these two proteins. The results of these assays indicate that the N-terminus of ezrin binds directly to paxillin, *in vitro*. This finding is not unanticipated because, as stated previously, the N-terminus of merlin has been shown to bind directly to paxillin (Fernandez-Valle et al., 2002). Additionally, merlin and ezrin, as family members, exhibit 61% identity between their FERM domains (Turunen et al., 1998) and are therefore expected to share at least some binding partners. Consistent with this supposition, research shows that merlin and ezrin do bind to several common proteins such as CD44 and RhoGDI (Sainio et al., 1997; Takahashi et al., 1997).

Although merlin and ezrin, as well as the other ERMs, have been shown to form head-to-tail associations, limited research is available hypothesizing the possible functions of these various heterodimers. Competitive binding studies demonstrate that the C-ERMAD of merlin has a higher affinity for the N-ERMAD of ezrin than for its own N-terminus (Nguyen et al., 2001). Research demonstrates that the N-terminus of ezrin binds directly to the cytoplasmic domain of CD44, an integral membrane protein (Hirao et al., 1996), and immunofluorescence microscopy has revealed that merlin colocalizes

with ezrin and CD44 beneath the cell membrane (Sainio et al., 1997). Additionally, recent research indicates that merlin-ezrin heterodimerization is promoted by activated PKA phosphorylation of merlin at S518 (Alfthan et al., 2004).

Proposed Model of Merlin/Paxillin/β1 Integrin/Ezrin Interactions

Based on the research cited, and coupled with the results presented in this thesis, it could be theorized that paxillin acts as a scaffold bringing ezrin and merlin into close proximity, through direct binding to both proteins, whereby the PKA-mediated phosphorylation of merlin at S518 promotes their heterodimerization. In this scenario, paxillin also function as a shuttle transporting the merlin-ezrin complex, via its LD3 motif binding to merlin PBD1, to the plasma membrane. This then positions, by way of their head-to-tail association, the N-terminus of ezrin for binding to CD44 and the C-terminus of merlin for binding to the β1 integrin cytoplasmic domain. As depicted in Figure 23, the proposed interactions between merlin, paxillin, β1 integrin, and ezrin result in the formation of a signaling complex coordinating both Schwann cell proliferation and motility. Additional *in vivo* research, such as immunofluorence staining and localization studies, should be conducted to further support the model presented in this thesis.

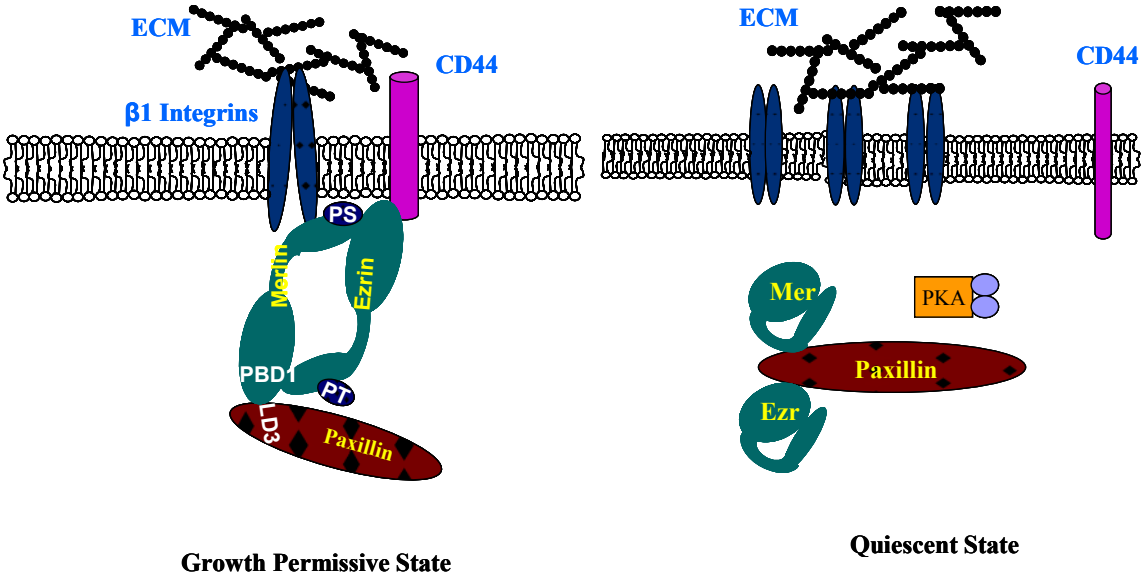

Figure 23. Model of Merlin/Paxillin/β1 Integrin/Ezrin Interactions in Proliferating and Quiescent Schwann Cells.
Our laboratory has proposed that, in quiescent Schwann cells, paxillin binds to merlin through its C-terminal PBD2 domain and removes merlin from the membrane (Fernandez-Valle *et al.*, 2002). Adding to this model, the results presented in this thesis suggest that the N-terminus of ezrin also binds to paxillin, bringing merlin and ezrin into close proximity (right panel). As cAMP levels increase, activated PKA phosphorylates merlin at S518 promoting the heterodimerization between merlin and ezrin. The merlin/ezrin complex is then shuttled to the plasma membrane by paxillin, through binding of its LD3 motif to merlin's PBD1 domain. At the membrane, the C-terminus of the merlin then binds to β1 integrin and the N-terminus of ezrin binds to CD44, resulting in the formation of a signaling complex coordinating both cell motility and proliferation (left panel).

REFERENCES

Albelda, S. M. & Buck, C. A. (1990). Integrins and other cell adhesion molecules. Federation of American Societies for Experimental Biology, 4 (11), 2868-2880.

Alfthan, K., Heiska, L., Grönholm, M., Renkema, H., & Carpén, O. (2004). Cyclic AMP-dependent protein kinase phosphorylates merlin at serine 518 independently of p21-activated kinase and promotes merlin-ezrin heterodimerization. The Journal of Biological Chemistry, 279 (18), 18559-18566.

Bach, I. (2000). The LIM domain: regulation by association. Mechanisms of Development, 91, 5-17.

Barret, C., Roy, C., Montcourrier, P., Mangeat, P., & Niggli, V. (2000). Mutagenesis of the phophatidylinositol 4,5-bisphosphate (PIP_2) binding site in the NH_2-terminal domain of ezrin correlates with its altered cellular distribution. The Journal of Cell Biology, 151, 1067-1080.

Bianchi, A. B., Hara, T., Ramesh, V., Gao, J., Klein-Szanto, A. J., Morin, F., Menon, A. G., Trofatter, J. A., Gusella, J. F., Seizinger, B. R., & Kley, N. (1994). Mutations in transcript isoforms of the neurofibromatosis 2 gene in multiple human tumour types. Nature Genetics, 6 (2), 185-192.

Brault, E., Gautreau, A., Lamarine, M., Callebaut, I., Thomas, G., & Goutebroze, L. (2001). Normal membrane localization and actin association of the NF2 tumor suppressor protein are dependent on folding of its N-terminal domain. Journal of Cell Science, 114, 1901-1912.

Bretscher, A., Chambers, D., Nguyen, R., & Reczek, D. (2000). ERM-Merlin and EBP50 protein families in plasma membrane organization and function. Annual Review of Cell and Developmental Biology, 16, 113-143.

Bretscher, A., Edwards, K., & Fehon, R. G. (2002). ERM proteins and merlin: integrators at the cell cortex. Nature Reviews: Molecular Cell Biology, 3, 586-599.

Brockes, J. P., Fields, K. L., & Raff, M. C. (1979). Studies on cultured rat Schwann cells. I. Establishment of purified populations from cultures of peripheral nerve. Brain Research, 165 (1), 105-118.

Brockes, J. P., Breakefield, X. O., & Martuza, R. L. (1986). Glial growth factor-like activity in Schwann cell tumors. Annals of Neurology, 20, 317-322.

Brown, M. C., Perrotta, J. A., & Turner, C. E. (1996). Identification of LIM3 as the principal determinant of paxillin focal adhesion localization and characterization of a novel motif on paxillin directing vinculin and focal adhesion kinase binding. The Journal of Cell Biology, 135 (4), 1109-1123.

Brown, M. C., Perrotta, J. A., & Turner, C. E. (1998). Serine and threonine phosphorylation of the paxillin LIM domains regulates paxillin focal adhesion localization and cell adhesion to fibronection. Molecular Biology of the Cell, 9, 1803-1816.

Brown, M. C., Curtis, M. S., & Turner, C. E. (1998). Paxillin LD motifs may define a new family of protein recognition domains. Nature Structural Biology, 5 (8), 677-678.

Brown, M. C. & Turner, C. E. (2004). Paxillin: adapting to change. Physiological Reviews, 84, 1315-1339.

Bunge, R. P. & Fernandez-Valle, C. (1995). Basic biology of the schwann cell. *In*: Neuroglia. Kettenmann, H., & Ranson, B., eds. New York, 44-57.

Burridge, K. & Chrzanowska-Wodnicka, M. (1996). Focal adhesions, contractility, and signaling. Annual Review of Cell and Developmental Biology, 12, 463-519.

Calderwood, D. A., Zent, R., Grant, R., Rees, D. J. G., Hynes, R. O., & Ginsberg, M. H. (1999). The talin head domain binds to integrin β subunit cytoplasmic tails and regulates integrin activation. The Journal of Biological Chemistry, 274 (40), 28071-28074.

Chen, L., Bailey, D., & Fernandez-Valle, C. (2000). Association of β1 integrin with focal adhesion kinase and paxillin in differentiating Schwann cells. Journal of Neuroscience, 20 (10), 3776-3784.

Chishti, A. H., Kim, A. C., Marfatia, S. M., Lutchman, M., Hanspal, M., Jindal, H., Liu, S.-C., Low, P. S., Rouleau, G. A., Mohandas, N., Chasis, J. A., Conboy, J. G., Gascard, P., Takakuwa, Y., Huang, S.-C., Benz, Jr, E. J., Bretscher, A., Fehon, R. G., Gusella, J. F., Ramesh, V., Solomon, F., Marchesi, V. T., Tsukita, Sh., Tsukita, Sa., Arpin, M., Louvard, D., Tonks, N. K., Anderson, J. M., Fanning, A. S., Bryant, P. J., Woods, D. F., & Hoover, K. B. (1998). The FERM domain: a unique module involved in the linkage of cytoplasmic proteins to the membrane. Trends in Biochemical Science, 23, 281-282.

Côté, J.-F., Turner, C. E., & Tremblay, M. L. (1999). Intact LIM3 and LIM4 domains of paxillin are required for the association to a novel polyproline region (Pro2) of protein-tyrosine phosphatase-PEST. The Journal of Biological Chemistry, 274 (29), 20550-20560.

Deguen, B., Mérel, P., Goutebroze, L., Giovannini, M., Reggio, H., Arpin, M., & Thomas, G. (1998). Impaired interaction of naturally occurring mutant NF2 protein with actin-based cytoskeleton and membrane. Human Molecular Genetics, 7 (2), 217-226.

den Bakker, M. A., Riegman, P. H. J., Suurmeijer, A. P., Vissers, C. J., Sainio, M., Carpén, O., & Zwarthoff, E. C. (2000). Evidence for a cytoskeleton attachment domain at the N-terminus of the NF2 protein. Journal of Neuroscience Research, 62, 764-771.

Dumanski, J. P., Carlbom, E., Collins, V. P., & Nordenskjöld, M. (1987). Deletion mapping of a locus on human chromosome 22 involved in the oncogenesis of meningioma. Proceedings of the National Academy of Sciences, USA, 84, 9275-9279.

Feltri, M. L., Porta, D. G., Prevatali, S. C., Modari, A., Migliavacca, B., Cassetti, A., Littlewood-Evans, A., Reichardt, L. F., Messing, A., Quattrini, A., Mueller, U., & Wrabetz, L. (2002). Conditional disruption of β1 integrin in Schwann cells impedes interaction with axons. The Journal of Cell Biology, 156 (1), 199-209.

Fernandez-Valle, C., Gwynn, L., Wood, P. M., Carbonetto, S., & Bunge, M. (1994). Anti-β1 integrin antibody inhibits Schwann cell myelination. Journal of Neurobiology, 25 (10), 1207-1226.

Fernandez-Valle, C., Tang, Y., Ricard, J., Rodenas-Ruano, A., Taylor, A., Hackler, E., Biggerstaff, J., & Iacovelli, J. (2002). Paxillin binds schwannomin and regulates its density-dependent localization and effect on cell morphology. Nature Genetics, 31 (4), 354-362.

Frazer, K. A., Boehnke, M., Budarf, M. L., Wolff, R. K., Emanuel, B. S., Myers, R. M., & Cox, D. R. (1992). A radiation hybrid map of the region on human chromosome 22 containing the neurofibromatosis type 2 locus. Genomics, 14 (3), 574-584.

Garratt, A. N., Voiculescu, O., Topilko, P., Charnay, P., & Birchmeier, C. (2000). A dual role of *erbB2* in myelination and in expansion of the schwann cell precursor pool. The Journal of Cell Biology, 148 (5), 1035-1046.

Gary, R. & Bretscher, A. (1995). Ezrin self-association involves binding of an N-terminal domain to a normally masked C-terminal domain that includes the F-actin binding site. Molecular Biology of the Cell, 6 (8), 1061-1075.

Gautreau, A., Louvard, D., & Arpin, M. (2002). ERM proteins and NF2 tumor suppressor: the yin and yang of cortical actin organization and cell growth signaling. Current Opinion in Cell Biology, 14, 104-109.

Gonzalez-Agosti, C., Xu, L., Pinney, D., Beauchamp, R., Hobbs, W., Gusella, J., & Ramesh, V. (1996). The merlin tumor suppressor localizes preferentially in membrane ruffles. Oncogene, 13, 1239-1247.

Gonzalez-Agosti, C., Wiederhold, T., Herndon, M. E., Gusella, J., & Ramesh, V. (1999). Interdomain interaction of merlin isoforms and its influence on intermolecular binding to NHE-RF. The Journal of Biological Chemistry, 274 (48), 34438-34442.

Grönholm, M., Sainio, M., Zhao, F., Heiska, L., Vahare, A., & Carpén, O. (1999). Homotypic and heterotypic interaction of the neurofibromatosis 2 tumor suppressor protein merlin and the ERM protein ezrin. Journal of Cell Science, 112, 895-904.

Gusella, J. F., Ramesh, V., MacCollin, M., & Jacoby, L. B. (1996). Neurofibromatosis 2: loss of merlin's protective spell. Current Opinion in Genetics & Development, 6, 87-92.

Gusella, J. F., Ramesh, V., MacCollin, M., & Jacoby, L. B. (1999). Merlin: the neurofibromatosis 2 tumor suppressor. Biochimica et Biophysica Acta, 1423, M29-M36.

Gutamnn, D. H., Giordano, M. J., Fishbach, A. S., & Guha, A. (1997). Loss of merlin expression in sporadic meningiomas, ependymomas, and schwannomas. Neurology, 48, 267-270.

Gutmann, D. H., Geist, R. T., Xu, H., Kim, J. S., & Saporito-Irwin, S. (1998). Defects in neurofibromatosis 2 protein function can arise at multiple levels. Human Molecular Genetics, 7, 335-345.

Gutmann, D. H., Haipek, C. A., & Lu, K. H. (1999). Neurofibromatosis 2 tumor suppressor protein, merlin, forms two functionally important intramolecular associations. Journal of Neuroscience Research, 58, 706-716.

Gutmann, D. H. (2001). The neurofibromatoses: when less is more. Human Molecular Genetics, 10 (7), 747-755.

Haack, H. & Hynes, R. O. (2001). Integrin receptors are required for cell survival and proliferation during development of the peripheral glial lineage. Developmental Biology, 233, 38-55.

Herreros, L., Rodríguez-Fernández, J. L., Brown, M. C., Alonso-Lebrero, J. L., Cabañas, C., Sánchez-Madrid, F., Longo, N., Turner, C. E., & Sánchez-Mateos, P. (2000). Paxillin localizes to the lymphocyte microtubule organizing center and associates with the microtubule cytoskeleton. The Journal of Biological Chemistry, 275 (34), 26436-26440.

Hirao, M., Sato, N., Kondo, T., Yonemura, S., Monden, M., Sasaki, T., Takai, Y., Tsukita, Sh., & Tsukita, Sa. (1996). Regulation mechanism of ERM (ezrin/radixin/moesin) protein/plasma membrane association: possible involvement of phosphatidylinositol turnover and Rho-dependent signaling pathway. The Journal of Cell Biology, 135 (1), 37-51.

Hoellerer, M. K., Noble, M. E. M., Labesse, G., Campbell, I. D., Werner, J. M., & Arold, S. T. (2003). Molecular recognition of paxillin LD motifs by the focal adhesion targeting domain. Structure, 11, 1207-1217.

Hovens, C. M. & Kaye, A. H. (2001). The tumour suppressor protein NF2/merlin: the puzzle continues. Journal of Clinical Neuroscience, 8 (1), 4-7.

Hynes, R. O. (2002). Integrins: bidirectional, allosteric signaling machines. Cell, 110, 673-687.

Hynes, R. O. (2003). Changing partners. Science, 300, 755-756.

Jessen, K. R. & Mirsky, R. (2002). Signals that determine schwann cell identity. Journal of Anatomy, 200 (4), 367-376.

Kissil, J. L., Johnson, K. C., Eckman, M. S., & Jacks, T. (2002). Merlin phosphorylation by p21-activated kinase 2 and effects of phosphorylation on merlin localization. The Journal of Biological Chemistry, 277 (12), 10394-10399.

Kimura, Y., Saya, H., & Nakao, M. (2000). Calpain-dependent proteolysis of NF2 protein: involvement in schwannomas and meningiomas. Neuropathology, 20, 153-160.

Knezevic, I., Leisner, T. M., & Lam, S. C.-T. (1996). Direct binding of the platelet integrin $\alpha_{IIb}\beta_3$ (GPIIb-IIIa) to talin. The Journal of Biological Chemistry, 271 (27), 16416-16421.

LaJeunesse, D. R., McCartney, B. M. & Fehon, R. G. (1998). Structural analysis of *drosophila* merlin reveals functional domains important for growth control and subcellular localization. The Journal of Cell Biology, 141 (7), 1589-1599.

Lamorte, L., Rodrigues, S., Sangwan, V., Turner, C. E., & Park, M. (2003). Crk associates with a multimolecular paxillin/GIT2/beta-PIX complex and promotes Rac-dependent relocalization of paxillin to focal contacts. Molecular Biology of the Cell, 14 (7), 2818-2831.

Lee, J. W. & Juliano, R. L. (2002). The α5β1 integrin selectively enhances epidermal growth factor signaling to the phosphatidylinositol-3-kinase/Akt pathway in intestinal epithelial cells. Biochimica et Biophysica Acta, 1542, 23-31.

Liddington, R. C. (2002). Will the real integrin please stand up? Structure, 10, 605-607.

Liu, S., Calderwood, D. A., & Ginsberg, M. H. (2000). Integrin cytoplasmic domain-binding proteins. Journal of Cell Science, 113, 3563-3571.

Lutchman, M. & Rouleau, G. A. (1996). Neurofibromatosis type 2: a new mechanism of tumor suppression. Trends in Neurosciences, 19 (9), 373-377.

Martel, V., Vignoud, L., Dupé, S., Frachet, P., Block, M. R., & Albigès-Rizo, C. (2000). Talin controls the exit of the integrin α5β1 from an early compartment of the secretory pathway. Journal of Cell Science, 113, 1951-1961.

Martin, T. A., Harrison, G., Mansel, R. E., & Jiang, W. G. (2003). The role of the CD44/ezrin complex in cancer metastasis. Critical Reviews in Oncology/Hematology, 46, 165-186.

Martuza, R. L & Eldridge, R. (1988). Neurofibromatosis 2. The New England Journal of Medicine, 318 (11), 684-688.

Matsui, T., Maeda, M., Doi, Y., Yonemura, S., Amano, M., Kaibuchi, K., Tsukita, Sa., & Tsukita, Sh. (1998). Rho-kinase phosphorylates COOH-terminal threonines of ezrin/radixin/moesin (ERM) proteins and regulates their head-to-tail association. The Journal of Cell Biology, 140 (3), 647-657.

Matsui, T., Yonemura, S, Tsukita, S., & Tsukita, S. (1999). Activation of ERM proteins *in vivo* by Rho involves phosphatidyl-inositol 4-phosphate 5-kinase and not ROCK kinases. Current Biology, 9, 1259-1262.

Maurel, P. & Salzer, J. L. (2000). Axonal regulation of Schwann cell proliferation and survival and the initial events of myelination requires PI 3-kinase activity. The Journal of Neuroscience, 20 (12), 4635-4645.

Meyer, D. & Birchmeier, C. (1995). Multiple essential functions of neuregulin in development. Nature, 378, 386-390.

Mirsky, R., Jessen, K. R., Brennan, A., Parkinson, D., Dong, Z., Meier, C., Parmantier, E., & Lawson, D. (2002). Schwann cells as regulators of nerve development. Journal of Physiology, 96, 17-24.

Narod, S. A., Parry, D. M., Parboosingh, J., Lenoir, G. M., Ruttledge, M., Fischer, G., Eldridge, R., Martuza, R. L., Frontali, M., Haines, J. L., Gusella, J. F., & Rouleau, G. A. (1992). Neurofibromatosis type 2 appears to be a genetically homogeneous disease. American Journal of Human Genetics, 51 (3), 486-496.

Nguyen, R., Reczek, D., & Bretscher, A. (2001). Hierarchy of merlin and ezrin N- and C-terminal domain interactions in homo- and heterotypic associations and their relationship to binding of scaffolding proteins EBP50 and E3KARP. The Journal of Biological Chemistry, 276 (10), 7621-7629.

Nikolopoulos, S. N. & Turner, C. E. (2000). Actopaxin, a new focal adhesion protein that binds paxillin LD motifs and actin and regulates cell adhesion. The Journal of Cell Biology, 151 (7), 1435-1447.

Nikolopoulos, S. N. & Turner, C. E. (2001). Integrin-linked kinase (ILK) binding to paxillin LD1 motif regulates ILK localization to focal adhesions. The Journal of Biological Chemistry, 276 (26), 23499-23505.

Obremski, V. J., Hall, A. M., & Fernandez-Valle, C. (1998). Merlin , the neurofibromatosis type 2 gene product, and β1 integrin associate in isolated and differentiating Schwann cells. Journal of Neurobiology, 37, 487-501.

Patil, S., Jedsadayanmata, A., Wencel-Drake, J. D., Wang, W., Knezevic, I., & Lam, S. C.-T. (1999). Identification of a talin-binding site in the integrin β3 subunit distinct from the NPLY regulatory motif of post-ligand binding functions. The Journal of Biological Chemistry, 274 (40), 28575-28583.

Pearson, M. A., Reczek, D., Bretscher, A., & Karplus, P. A. (2000). Structure of the ERM protein moesin reveals the FERM domain fold masked by an extended actin binding tail domain. Cell, 101, 259-270.

Previtali, S., Feltri, M. L., Archelos, J. J., Quattrini, A., Wrabetz, L., & Hartung, H.-P. (2001). Role of integrins in the peripheral nervous system. Progress in Neurobiology, 64, 35-49.

Pfaff, M., Liu, S., Erle, D. J., & Ginsberg, M. H. (1998). Integrin β cytoplasmic domains differentially bind to cytoskeletal proteins. The Journal of Biological Chemistry, 273 (11), 6104-6109.

Pykett, M. J., Murphy, M., Harnish, P. R., & George, D. L. (1994). The neurofibromatosis 2 (NF2) tumor suppressor gene encodes multiple alternatively spliced transcripts. Human Molecular Genetics, 3 (4), 559-564.

Rong, R., Surace, E. I., Haipek, C. A., Gutmann, D. H., & Ye, K. (2004). Serin 518 phosphorylation modulates merlin intramolecular association and binding to critical effectors important for NF2 growth suppression. Oncogene, 23 (52), 8447-8454.

Rouleau, G. A., Wertelecki, W., Haines, J. L., Hobbs, W. J., Trofatter, J. A., Seizinger, B. R., Martuza, R. L., Superneau, D. W., Conneally, P. M., & Gusella, J. F. (1987). Genetic linkage of bilateral acoustic neurofibromatosis to a DNA marker on chromosome 22. Nature, 329, 246-248.

Rouleau, G. A., Seizinger, B. R., Wertelecki, W., Haines, J. L., Superneau, D. W., Martuza, R. L., & Gusella, J. F. (1990). Flanking markers bracket the neurofibromatosis type 2 (NF2) gene on chromosome 22. American Journal of Human Genetics, 46, 323-328.

Rouleau, G. A., Merel, P., Lutchman, M., Sanson, M., Zucman, J., Marineau, C., Hoang-Xaun, K., Demczuk, S., Desmaze, C., Plougastel, B., Pulst, S. M., Lenoir, G., Bijlsma, E., Fashold, R., Dumanski, J., de Jong, P., Parry, D., Eldridge, R., Aurias, A., Delattre, O., & Thomas, G. (1993). Alteration in a new gene encoding a putative membrane-organizing protein causes neuro-fibromatosis type 2. Nature, 363, 515-521.

Ruggieri, M. & Huson, S. M. (1999). The neurofibromatoses. An overview. Italian Journal of Neurological Science, 20, 89-108.

Sainio, M., Zhao, F., Heiska, L., Turunen, O., den Bakker, M., Zwarthoff, E., Lutchman, M., Rouleau, G. A., Jääskeläinen, J., Vaheri, A., & Carpén, O. (1997). Neurofibromatosis 2 tumor suppressor protein colocalizes with ezrin and CD44 and associates with actin-containing cytoskeleton. Journal of Cell Science, 110, 2249-2260.

Sainio, M., Jääskeläinen, J., Pihlaja, H. & Carpén, O. (2000). Mild familial neurofibromatosis 2 associates with expression of merlin with altered COOH-terminus. Neurology, 54, 1132-1138.

Sastry, S. K. & Burridge, K. (2000). Focal adhesions: a nexus for intracellular signaling and cytoskeletal dynamics. Experimental Cell Research, 261, 25-36.

Schaller, M. D., Otey, C. A., Hildebrand, J. D., & Parsons, J. T. (1995). Focal adhesion kinase and paxillin bind to peptides mimicking β integrin cytoplasmic domains. The Journal of Cell Biology, 130 (5), 1181-1187.

Schaller, M. D. (2001). Paxillin: a focal adhesion-associated adaptor protein. Oncogene, 20, 6459-6472.

Scherer, S. S. (2002). Myelination: some receptors required. The Journal of Cell Biology, 156 (1), 13-15.

Schlaepfer, D. D., Hauck, C. R., & Sieg, D., J. (1999). Signaling through focal adhesion kinase. Progress in Biophysics & Molecular Biology, 71, 435-478.

Schuppan, D., Somasundaram, R., Dieterich, W., Ehnis, T., & Bauer, M. (1994). The extracellular matrix in cellular proliferation and differentiation Annals New York Academy of Sciences, 733, 87-102.

Scoles, D. R., Chen, M., & Pulst, S.-M. (2002). Effects of *Nf2* missense mutations on schwannomin interactions. Biochemical and Biophysical Research Communications, 290, 366-374.

Seizinger, B. R., Martuza, R. L., & Gusella, J. F. (1986). Loss of genes on chromosome 22 in tumorigenesis of human acoustic neuroma. Nature, 322 (6080), 644-647.

Seizinger, B. R., De La Monte, S., Atkins, L., Gusella, J. F., & Martuza, R. L. (1987a). Molecular genetic approach to human meningioma: Loss of genes on chromosome 22. Proceedings of the National Academy of Sciences, USA, 84, 5419-5423.

Seizinger, B. R., Rouleau, G., Ozelius, L. J., Lane, A. H., St. George-Hyslop, P., Huson, S., Gusella, J. F., & Martuza, R. L. (1987b). Common pathogenetic mechanism for three tumor types in bilateral acoustic neurofibromatosis. Science, 236 (4799), 317-319.

Shaw, R. J., McClatchey, A. I., & Jacks, T. (1998b). Regulation of the neurofibromatosis type 2 tumor suppressor protein, merlin, by adhesion and growth arrest stimuli. The Journal of Biological Chemistry, 273 (13), 7757-7764.

Shaw, R. J., Paez, J. G., Curto, M., Yaktine, A., Pruitt, W. M., Saotome, I., O'Bryan, J. P., Gupta, V., Ratner, N., Der, C. J., Jacks, T., & McClatchey, A.I. (2001). The *NF2* tumor suppressor, merlin, functions in rac-dependent signaling. Developmental Cell, 1, 63-72.

Shen, Y., Schneider, G., Cloutier, J.-F., Veillette, A., & Schaller, M. D. (1998). Direct association of protein-tyrosine phosphatase PTP-PEST with paxillin. The Journal of Biological Chemistry, 273 (11), 6474-6481.

Sherman, L., Xu, H., Geist, R. T., Saporito-Irwin, S., Howells, N., Ponta, H., Herrlich, P., & Gutmann, D. H. (1997). Interdomain binding mediates tumor growth suppression by the *NF2* gene product. Oncogene, 15, 2505-2509.

Shimizu, T., Seto, A., Maita, N., Hamada, K., Tsukita, Sh., Tsukita, Sa., & Hakoshima, T. (2002). Structural basis for neurofibromatosis type 2. The Journal of Biological Chemistry, 277 (12), 10332-10336.

Simons, P. C., Pietromonaco, S. F., Reczek, D., Bretscher, A., & Elias, L. (1998). C-terminal threonine phosphorylation activates ERM proteins to link the cell's cortical lipid bilayer to the cytoskeleton. Biochemical and Biophysical Research Communications, 253, 561-565.

Smith, W. J., Nassar, N., Bretscher, A., Cerione, R. A., & Karplus, P. A. (2003). Structure of the active N-terminal domain of ezrin. The Journal of Biological Chemistry, 278 (7), 4949-4956.

Sun, C., Robb, V. A., & Gutmann, D. H. (2002). Protein 4.1 tumor suppressors: getting a FERM grip on growth regulation. Journal of Cell Science, 115, 3991-4000.

Takahashi, K., Sasaki, T., Mammoto, A., Takaishi, K., Kameyama, T., Tsukita, Sa., Tsukita, Sh., & Takai, Y. (1997). Direct interaction of the Rho GDP dissociation inhibitor with ezrin/radixin/moesin initiates the activation of the small Rho G protein. The Journal of Biological Chemistry, 272 (37), 23371-23375.

Taylor, A. R., Geden, S. E., & Fernandez-Valle, C. (2003). Formation of a β1 integrin signaling complex in Schwann cells is independent of Rho. GLIA, 41, 94-104.

Trofatter, J. A., MacCollin, M. M., Rutter, J. L., Murrell, J. R., Duyao, M. P., Parry, D. M., Eldridge, R., Kley, N., Menon, A. G., Pulaski, K., Haase, V. H., Ambrose, C. M., Munroe, D., Bove, C., Haines, J. L., Martuza, R. L., MacDonald, M. E., Seizinger, B. R., Short, M. P., Buckler, A. J., & Gusella, J. F. (1993). A novel moesin-, ezrin-, radixin-like gene is a candidate for the neurofibromatosis 2 tumor supressor. Cell, 72, 791-800.

Tsukita, S. & Yonemura, S. (1999). Cortical actin organization: lessons from ERM (Ezrin/Radixin/Moesin) proteins. The Journal of Biological Chemistry, 274 (49), 34507-34510.

Tumbarello, D. A., Brown, M. C., & Turner, C. E. (2002). The paxillin LD motifs. Federation of European Biochemical Societies Letters, 513, 114-118.

Turner, C. E. & Miller, J. T. (1994). Primary sequence of paxillin contains putative SH2 and SH3 domain binding motifs and multiple LIM domains: identification of a vinculin and pp125^{FAK}-binding region. Journal of Cell Science, 107, 1583-1591.

Turner, C. E, Brown, M. C., Perrotta, J. A., Riedy, M. C., Nikolopoulos, S. N., McDonald, A. R., Bagrodia, S., Thomas, S., & Leventhal, P. S. (1999). Paxillin LD4 motif binds PAK and PIX through a novel 95-kD ankyrin repeat, ARF-GAP protein: a role in cytoskeletal remodeling. The Journal of Cell Biology, 145 (4), 851-863.

Turner, C. E. (2000). Paxillin and focal adhesion signaling. Nature Cell Biology, 2 (12), E231-E236.

Turner, C. E. (2000). Paxillin interactions. Journal of Cell Science, 13 (Pt23), 4139-4140.

Turunen, O., Sainio, M., Jääskeläinen, J., Carpén, O., & Vaheri, A. (1998). Structure-function relationships in the ezrin family and the effect of tumor-associated point mutations in neurofibromatosis 2 protein. Biochimica et Biophysica Acta, 1387, 1-16.

Wagner, A. L. (2003). Neurofibromatosis Type 2. Retrieved June 1, 2005, from http://www.emedicine.com/radio/topic475.htm.

Wertelecki, W., Rouleau, G. A., Superneau, D. W., Forehand L. W., Williams, J. P., Haines, J. L., & Gusella, J. F. (1988). Neurofibromatosis 2: clinical and DNA linkage studies of a large kindred. New England Journal of Medicine, 319 (5), 278-283.

Wolff, R. K., Frazer, K. A., Jackler, R. K., Lanser, M. J., Pitts, L. H., & Cox, D. R. (1992). Analysis of chromosome 22 deletions in neurofibromatosis type 2-related tumors. American Journal of Human Genetics, 51 (3), 478-485.

Woodrow, M. A., Woods, D., Cherwinski, H. M., Stokoe, D., & McMahon, M. (2003). Ras-induced serine phosphorylation of the focal adhesion protein paxillin is mediated by the Raf→MEK→ERK pathway. Experimental Cell Research, 287, 325-338.

Xiao, G., Chernoff, J., & Testa, J. R. (2003). *NF2*: The wizardry of merlin. Genes, Chromosomes & Cancer, 38, 389-399.

Xing, B., Jedsadayanmata, A., & Lam, S. C.-T. (2001). Localization of an integrin binding site to the C terminus of talin. The Journal of Biological Chemistry, 276 (48), 44373-44378.

Xu, H. & Gutmann, D. H. (1998). Merlin differentially associates with the microtubule and actin cytoskeleton. Journal of Neuroscience Research, 51, 403-415.

Yan, B., Calderwood, D. A., Yaspan, B., & Ginsberg, M. H. (2001). Calpain cleavage promotes talin binding to the β3 integrin cytoplasmic domain. The Journal of Biological Chemistry, 276 (30), 28164-28170.

Zanazzi, G., Einheber, S., Westreich, R., Hannocks, M., Bedell-Hogan, D., Marchionni, M. A., & Salzer, J. L. (2001). Glial growth factor/neuregulin inhibits Schwann cell myelination and induces demyelination. The Journal of Cell Biology, 152 (6), 1289-1299.